Characterization of Acetate Metabolism Genes in *Sinorhizobium* (*Rhizobium*) *meliloti*

Fathuma Zuleikha Thaha

Department of Natural Resource Sciences
McGill University
Montréal, Canada

July, 1999

A thesis submitted to the
Faculty of Graduate Studies and Research
in partial fulfillment of the requirements of the degree of
Master of Science

ABSTRACT

Fifteen mutants of *Sinorhizobium* (*Rhizobium*) *meliloti* unable to utilize acetate as a sole carbon source (Ace$^-$) were characterized in this study. Merodiploid complementation tests showed that nine of these mutations were in loci distinct from previously described gluconeogenic loci. The chromosomal locations of the mutations were determined, and complementing clones were isolated from the cosmid library of *S. meliloti* genomic DNA. The mutants were placed into four groups (I-IV) based on genetic linkage in phage co-transduction. None of the mutations were in glyoxylate shunt enzyme-encoding genes. Nucleotide sequence analysis of *ace* mutants from Groups III and IV showed mutations in genes encoding acetyl-CoA synthetase *(acsB)* and anaerobic coproporphyrinogen III oxidase (*hemN*) respectively. Cell extracts of the *hemN* mutant exhibited double the isocitrate lyase levels of the wild type. The *acsB* mutant lacked acetyl-CoA synthetase activity and had an interesting growth phenotype; it was able to grow on low concentrations of acetate only. Previous DNA sequence analysis in our laboratory had determined that Group II mutants had mutations located within the *pod* gene, encoding the enzyme pyruvate orthophosphate dikinase. The Ace$^-$ phenotype contrasts with the Ace$^+$ phenotype of a *pod* mutant isolated by Østerås et al. (Microbiology. **143**:1639-1648, 1997). The *pod* gene was reported to be required for the suppression of the succinate utilization phenotype of a *pckA* mutant. In the present study, we have demonstrated that *spk*, the second site suppressor of *pckA*, is tightly linked to *pod*, but is in fact a distinct locus. Expression analysis of a *pod*::*lacZ* gene fusion indicated that the expression of the *pod* gene does not depend on growth phase or carbon source. The wild-type *pod* cosmid clone is able to suppress the succinate phenotype of the *pckA* mutant. The role of *pod* in *pckA* suppression is yet to be determined. This study identified three genes involved in acetate metabolism and indicates that the mechanisms used to metabolize acetate in *S. meliloti* are probably different from that used by enterics.

RÉSUMÉ

Quinze mutants de *Sinorhizobium* (*Rhizobium*) *meliloti* incapables d'utiliser l'acétate comme unique source de carbone (Ace$^-$) ont été characterisé dans cette étude. Des tests de complémentation mérodiploide ont démontré que neuf de ces mutations étaient localisés dans des loci distincts de ceux préalablement décrits; les loci gluconéogéniques. Les mutations ont été cartographié au chromosome et des clones permettant un complémentation ont été isolés à partir de la banque de cosmides d'ADN génomique de *S. meliloti*. Les mutants ont été répartis dans quatre groupes (I-IV) basés sur la proximité génétique lors de la co-transduction par les phages. Aucune des mutations n'affectait les gènes codant pour ces enzymes du cycle du glyoxylate. L'analyse de la séquence nucléotique des mutants *ace* des groupes III et IV a montré des mutations dans des gènes codant pour l' acetyl-CoA synthétase (*acsB*) et l'oxidase anaérobique coproporphyrinogène III (*hemN*) respectivement. Des extraits cellulaire des mutants *hemN* ont démontré des taux d'isoctrate lyase doubles par rapport à la sorte sauvage. Le mutant *acsB* était dépourvu d'activité de l' acetyl-CoA synthétase et présentait un phénotype de croissance intéressante - il était capable de croître sur des concentrations très basses d'acétate seulement. Des analyses antérieures de séquence d'ADN effectuées dans notre laboratoire ont démontré que le groupe II avait des mutations localisées à l'intérieur du gène *pod*, codant par la pyruvate orthophosphate dikinase. Le phénotype Ace$^-$ contraste avec le phénotype Ace$^+$ d'un mutant *pod* isolé par Østerås et al. (Microbiology. **143**:1639-1648, 1997). Ce gène *pod* a été rapporté comme étant nécessaire pour la suppression du phénotype d'utilisation du succinate chez un mutant *pckA*. Dans la présente étude, nous avons démontré que le gène *pod* est étroitment relié à l'allele supprimante mais dans un locus différent. Ceci peut expliquer les différents phénotypes observés dans les deux études. L'analyse de l'expression du gène fusion *pod*::*lacZ* indique que celle du gène *pod* ne dépend pas de la phase de croissance ni de la source de carbone. Notre clone cosmide de type sauvage *pod* est capable de supprimer le phénotype de succinate du mutant *pckA*. Le role de *pod* dans la suppression de *pckA* reste cependant à déterminer. Cette étude a demontré qu'il existe trois gènes impliqués en

métabolisant l'acétate et que les mécanismes employés par *S. meliloti* pour métaboliser l'acétate sont probablement différents de cela employé par enterics.

ACKNOWLEDGEMENTS

I would like to thank Dr. T. C. Charles for giving me the opportunity to carry out this project, for his encouragement, keen guidance and supervision throughout this study and during the preparation of this thesis. I would also like to thank Dr. B. T. Driscoll and Dr. D. F. Niven for all the advice and constant encouragement. I really appreciate Dr. Driscoll's help and kindness in allowing me to use the computer in his office during the last stages of this work.

A big thanks to Punita Aneja and Guo-Qin Cai for always being there for me. I will always be grateful for the extraordinary help, patience, invaluable advice and friendship. I would like to thank Dr. Kirk Bartholomew, Tim Dumonceaux, Gary DosSantos, Dominic Frigon, all the other members of the Charles laboratory at Mac and at Waterloo, other graduate students at Mac, Rita Rivera and Dawn Brooks for all their help, peer support and friendly presence. Thanks to Julie Fortier for very kindly translating the abstract into French. I am grateful to Marie Kubecki for making sure that all the administrative work was taken care of and all the deadlines were met.

I would like to thank my parents, my brothers and sister for believing in me and for all their love, encouragement, patience and support. A special thank you to my fiancé and best friend Nabil for his love and understanding. I would also like to express my appreciation to Nabil's family for their warmth and support, especially during my stay in Waterloo.

Last but not least, financial support of Agriculture and Agri-Food Canada is gratefully acknowledged.

TABLE OF CONTENTS

LIST OF TABLES

LIST OF FIGURES

LIST OF ABBREVIATIONS

AACS	acetoacetyl-CoA synthetase
Ace	acetate
Ack	acetate kinase
ACS	acetyl-CoA synthetase enzyme
AcsA	acetoacetyl-CoA synthetase
AcsB	acetyl-CoA synthetase
ADP	adenosine diphosphate
AHAS	acetohydroxy acid synthase
ALS	alkaline lysing solution
AMP	adenosine monophosphate
Ap	ampicillin
ATP	adenosine triphosphate
bp	base pair(s)
cfu	colony forming units
Cm	chloramphenicol
CoA	coenzyme A
Da	dalton
DME	NAD^+-dependent malic enzyme
DNA	deoxyribonucleic acid
ED	Enter-Doudoroff
EDTA	ethylene diamine tetraacetic acid
EMP	Embden-Meyerhof-Parnos
ENO	enolase
FADH	reduced flavine adenine dinucleotide
GAP	glyceraldehyde-3-phosphate dehydrogenase
Gm	gentamicin
GTP	guanosine triphosphate
IDH	isocitrate dehydrogenase
kb	kilobase or kilobase pair

Km	kanamycin
LB	Luria Bertani
MDH	malate dehydrogenase
NAD	nicotinamide adenine dinucleotide
NADH	reduced nicotinamide adenine dinucleotide
NADP	nicotinamide adenine dinucleotide phosphate
Nm	neomycin
OAA	oxaloacetate
OD	optical density
ONPG	*o*-nitrophenyl-β-D-galactopyranoside
PCK	phosphoenolpyruvate carboxykinase
PEP	phosphoenolpyruvate
PGK	3-phosphoglycerate kinase
PHB	poly-β-hydroxybutyrate
PTA	inorganic phosphate
PPDK	pyruvate orthophosphate dikinase
Pta	phosphotransacetylase
PYC	pyruvate carboxylase
PYK	pyruvate kinase
Rf	rifampin
RNA	ribonucleic acid
SDS	sodium dodecyl sulphate
SE	standard error
Sm	streptomycin
Sp	spectinomycin
Tc	tetracycline
TCA	tricarboxylic acid
TME	$NADP^+$-dependent malic enzyme
Tris	tris (hydroxymethyl)amino methane
TY	tryptone yeast
UV	ultraviolet

X-Gal	5-bromo-4-chloro-3-indolyl-β-D-galactopyranoside

CHAPTER 1

INTRODUCTION AND LITERATURE REVIEW

INTRODUCTION

Legumes commonly form symbioses with species of the bacterial family *Rhizobiaceae*, which can result in an efficient biological nitrogen fixation. Such an association is useful to the host plant in nitrogen-limiting conditions. It is also advantageous to the bacteria. The nodules house them, and they also receive a steady supply of nutrients from the plant. Today, nitrogen-fixing crops rate third, behind cereals and root crops, in global food production from the land. Their importance is increasing as people move more seriously towards sustainable agriculture. There is a need for better agricultural systems with plants, technologies and microorganisms that are adapted to modern agricultural needs.

In order to enhance the performance of rhizobia, we need to have a good understanding of the association between the host plant and the bacterium. Major advances have recently been made towards understanding the metabolic pathways important for the bacterium (in the free-living and symbiotic state). Acetate, a two-carbon substrate, has been found in significant quantities in nodules, and may be used as a carbon and energy source by rhizobia in the free-living state. Acetyl-coenzyme A, a common metabolic form of acetate, is an intermediate in various anabolic and catabolic pathways. A study of acetate metabolism may therefore provide insights into the regulation of fluxes of carbon molecules into different metabolic pathways. This thesis is an effort to understand the metabolism of two-carbon compounds such as acetate in *Sinorhizobium* (*Rhizobium*) *meliloti*, a soil bacterium that forms nitrogen-fixing symbiosis with alfalfa and other medics that are important forage crops. This organism has been the focus of much research because of its well-developed genetic system.

LITERATURE REVIEW

Rhizobia

Rhizobia are Gram negative, rod-shaped bacteria that form nitrogen-fixing symbioses with leguminous plants. These bacteria include the genera *Rhizobium*, *Bradyrhizobium*, *Mesorhizobium*, *Sinorhizobium* and *Azorhizobium*. Most rhizobial species only nodulate specific hosts. For example *Sinorhizobium meliloti*, also called *Rhizobium meliloti*, forms symbioses with alfalfa, while *Bradyrhizobium japonicum* nodulates soybean. Rhizobia can also be metabolically divided into two classes - slow growers and fast growers. Fast growers (*S. meliloti*, *R. leguminosarum*, *R. leguminosarum* bv. *trifolii*) have a mean generation time of 2- 4 hours. Slow growers (*B. japonicum*, *R. lupini*) have a mean generation time of 6-8 hours (102).

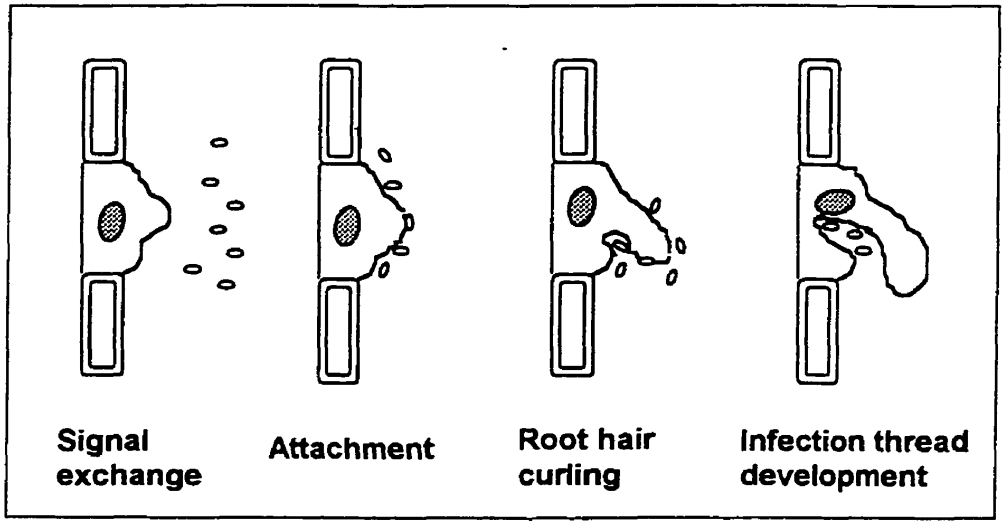

Figure 1.1. Early stages of root infection by Rhizobia (adapted from (88)).

Free-living rhizobia are generally unable to fix N_2. They can carry out this task only after colonizing the host plant. Plants secrete flavonoids into the rhizosphere (Figure 1.1). When the bacteria encounter the appropriate flavonoid, they respond by synthesizing and excreting Nod factors. This exchange of signals occurs as the bacteria

bind to specific sites on the root hairs. This stimulates the formation of an infection thread through which the bacteria are able to invade the plant. Cell division and cell growth in the plant root cortex leads to the formation of a root nodule in which bacteria infect host cells and differentiate into bacteroids that fix N_2.

Carbon and Nitrogen Metabolism

Bacteria supply their host with a nitrogen source, and the plant supplies the bacteria with a supply of carbon and energy. Even though ammonia has been thought to be the major N_2-containing compound supplied to hosts, there is recent evidence suggesting that the nitrogen source for soybean is likely alanine (115). N_2-fixation in this symbiotic association is an energy intensive process. The nitrogenase enzyme that catalyzes the reduction of N_2 requires at least 16 ATP and 8 reducing equivalents per mole of ammonia produced (51). Nitrogenase is readily and irreversibly inactivated by O_2. In the nodule, the oxygen concentration is regulated by leghaemoglobin synthesized by the host plant. Leghaemoglobin facilitates oxygen diffusion (for respiration) and maintains a low level of free oxygen in the bacteroid, so that nitrogenase is not inactivated (91).

The N_2-fixing capacity of the *Rhizobium*-legume symbiosis is influenced by the amount of photosynthate available to the bacteroid. C_4-dicarboxylic acids such as succinate, fumarate and malate are the primary energy source supplied by the plants to the bacteroid during N_2-fixation. Studies have shown that C_4-dicarboxylic acids are found in significant quantities in the nodule cytosol (113) and stimulate nitrogenase activity in isolated bacteroids(102). Mutants defective in dicarboxylic acid transport (Dct^- phenotype) are incapable of fixing N_2 (4, 36, 41, 92, 122).

When *S. meliloti* invades the nodule and differentiates from a free-living to a symbiotic state, it has to make extensive adjustments to its carbon and nitrogen metabolism. C_4-dicarboxylic acids appear to be metabolized via the tricarboxylic acid (TCA) cycle (Figure 1.2). The acids enter the TCA cycle as acetyl-CoA, which is synthesized from malate via the NAD^+-dependent malic enzyme and pyruvate dehydrogenase. The metabolism of the TCA cycle intermediates in rhizobia was recently

reviewed by Dunn (34). A functional TCA cycle is important for *Rhizobium* since strains that are defective in succinate dehydrogenase and α-ketoglutarate dehydrogenase form ineffective nodules. Mutants that are defective in the uptake of C_4-dicarboxylic acids are capable of forming an infection thread and invading the plant, indicating that C_4-dicarboxylic acids are not the likely source of carbon and energy for the invading bacteria.

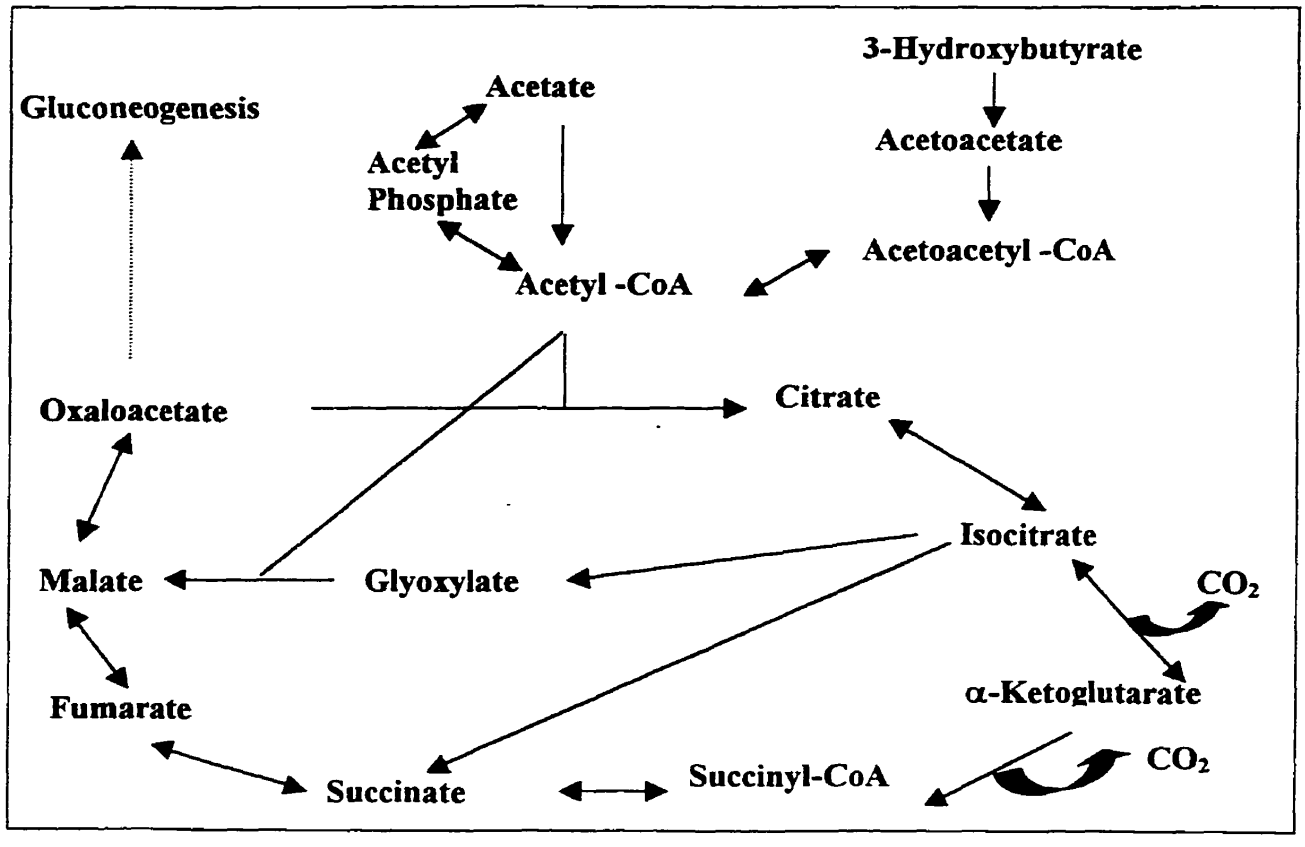

Figure 1.2. Tricarboxylic acid cycle and the glyoxylate bypass

Acetyl-CoA is the central metabolite found at the junction of various anabolic and catabolic pathways. Several pathways can be used to produce acetyl-CoA for entry into the TCA cycle. In *S. meliloti*, glucose is metabolized via the Entner Dourdoroff pathway, yielding two molecules of pyruvate -- one is converted to acetyl-CoA by pyruvate dehydrogenase and the other is converted to OAA by pyruvate carboxylase. Acetyl-CoA

may also be derived from poly-3-hydroxybutyrate (PHB). PHB is a bacterial storage compound that accumulates in the cell when growth is limited but when there is excess carbon. It can represent more than 50% of the cell dry weight in *S. meliloti* (110). It acts as a carbon and energy sink and allows bacterial cells to respond better to starvation and other stress conditions. PHB granules have been observed in the invading free-living *S. meliloti* but not in the bacteroid form (87). Therefore it is possible that PHB plays a role in *S. meliloti* infections. When PHB is degraded, it is depolymerized and oxidized to acetoacetate. Acetoacetate is converted to acetyl-CoA in two steps. Acetyl-CoA can also be synthesized from acetate and this is described later in the review.

Acetate Metabolism

Even though C_4-dicarboxylic acids are important energy-yielding compounds supplied by the host, the host may also supply organic acids and amino acids (77, 103). An organic acid that is found in large quantities in *B. japonicum* nodules is acetate (59). Several lines of evidence suggest that acetate may be used by *B. japonicum* bacteroids. Firstly, acetate readily diffuses across the peribacteroid membrane (112). Secondly, mature *B. japonicum* bacteroids have increased acetate uptake levels and high activities of acetate metabolism-related enzymes (99). When the genetics of acetate metabolism was studied in *Saccharomyces cerevisiae*, there were 3 major mutant groups. The mutants had defects in the glyoxylate shunt, TCA cycle, or gluconeogenesis (76). Gluconeogenesis is the pathway that converts TCA cycle intermediates, such as succinate and malate, to glucose. The glyoxylate shunt is a bypass of the TCA cycle, which converts isocitrate and acetyl-CoA to succinate and malate. Two other minor groups were also observed. One group included regulatory mutants and mutants with elevated levels of metabolic enzymes, and the other contained mutants with unknown defects. Studies have also indicated that inability of *Escherichia coli* and *Salmonella typhimurium* strains to utilize acetate as a sole carbon source may be caused by defects in the TCA cycle, gluconeogenesis and glyoxylate shunt (21, 24).

Acetate Auxotrophy

Acetohydroxy acid synthase (AHAS) is an essential enzyme for isoleucine and valine biosynthesis when *E. coli* K-12 and *S. typhimurium* strains are grown on either acetate or oleate as a carbon source (26, 27). *E. coli* has two AHAS enzymes, AHAS I and AHAS III, and these isozymes catalyze the synthesis of α-aceto-hydroxybutyrate and α-acetolactate. If *E. coli* is deficient in one of the AHAS, it can still make sufficient isoleucine and valine for growth on minimal media supplemented with carbon sources such as glucose and succinate (29). However it was found that AHAS I mutants do not make isoleucine and valine when they are grown on acetate and oleate (26). The authors suggest that the metabolic conditions that arise during growth on acetate (i.e. decrease in the intracellular concentration of pyruvate; increase in the level of glyoxylate) may decrease the activity of AHAS III below the level required for growth.

Acetate Utilization

The metabolic utilization of acetate, whether for lipid synthesis, amino acid synthesis or for oxidation via the TCA cycle, requires that it first be activated to acetyl-CoA. Two main pathways exist to bring about this conversion. In one mechanism, acetyl-CoA synthetase catalyzes the acetylation of CoA with the cleavage of ATP to give AMP and an inorganic pyrophosphate. In the second mechanism, two enzymes are involved.

$$\text{acetate} + \text{ATP} \xrightarrow{\text{acetate kinase}} \text{acetyl-phosphate} + \text{ADP}$$

$$\text{acetyl-phosphate} + \text{CoA} \xrightarrow{\text{phosphotransacetylase}} \text{acetyl-CoA} + \text{Pi}$$

ack and *pta* encode acetate kinase and phosphotransacetylase respectively. The two genes have been mapped in both *S. typhimurium* and *E. coli* near *purF* (69). These

two enzymes are not induced by acetate or subject to catabolite repression by glucose (12). In addition, these enzymes are active and operative under aerobic and anaerobic conditions. Acetyl-CoA synthetase in *E. coli*, on the other hand, is induced by acetate and subject to catabolite repression. The uptake of acetate occurs at a higher affinity but much lower V_{max} (12). According to Kumari, *ack* and *pta* mutants grow only on low concentrations of acetate (≤10 mM) (65). *acs* mutants, however, grow poorly at these concentrations (65).

Some organisms use only one of these pathways, while others use both. *E. coli* requires both pathways for optimal growth over a wide range of acetate concentrations (65). In *S. meliloti*, it is likely that both pathways are used since mutations in either *acs* or *ack* do not affect growth on acetate (15, 106). Sequence analysis indicates that the *S. meliloti acsA* gene encodes a putative protein of 71 kDa, with a structure similar to that of *E. coli* Acs (16). The *S. meliloti ack* and *pta* genes are located within an operon that also includes an unidentified ORF and another ORF that is likely *fabI* , and *ackA* and *ackA-pta* double mutants are not affected in nodulation or nitrogen fixation (105).

Glyoxylate Shunt

The TCA cycle is the only pathway for the complete oxidation of acetate. In addition to being a terminal pathway in respiration, the TCA cycle is also a source of important intermediates. For instance, oxaloacetate supplies the carbon skeleton for the synthesis of aspartate, which is the source of nitrogen for the amino acids methionine, lysine, threonine and isoleucine and the pyrimidine nucleic acids (64). With each turn of the TCA cycle, two carbon atoms are lost as CO_2, and therefore there is no net assimilation of carbon by acetyl-CoA when two-carbon compounds are the sole carbon source. Microorganisms have anaplerotic pathways that replenish cycle intermediates so that the TCA cycle can function when active biosynthesis is taking place. The glyoxylate shunt bypasses the two CO_2-evolving steps, and allows the synthesis and net accumulation of four-carbon compounds during growth on two-carbon substrates such as acetate, or acetyl-CoA from fatty acids. There are two oxidative steps involved in the

glyoxylate shunt – one during the conversion of pyruvate to acetyl-CoA (pyruvate dehydrogenase) and the other step when malate is converted to oxaloacetate (malate dehydrogenase). The glyoxylate shunt is able to provide some energy because at these oxidative steps, most of the cell energy is obtained from the simultaneous oxidation of other acetate molecules via the TCA cycle. Most of our current knowledge of the glyoxylate shunt comes from studies with *E. coli* (64, 74). The shunt is subject to catabolite repression, and therefore, whenever an easily metabolizeable carbon source like glucose or succinate becomes available, the bypass is turned off (94). Since the glyoxylate shunt is the most important pathway in acetate metabolism, the enzymes involved and its regulation will be discussed briefly.

Enzymes of the Glyoxylate Shunt

Malate synthase and isocitrate lyase

The two enzymes of the glyoxylate shunt are isocitrate lyase and malate synthase, encoded by the *aceA* and *aceB* genes respectively. The two enzymes catalyze the following reactions:

$$\text{isocitrate} \xrightarrow{\text{isocitrate lyase}} \text{succinate} + \text{glyoxylate}$$

$$\text{glyoxylate} + \text{acetyl-CoA} \xrightarrow{\text{malate synthase}} \text{malate} + \text{CoA}$$

The two enzymes were discovered in *E. coli* in the 1950's (64). Isocitrate lyase has molecular weight of 47,000 and malate synthase a molecular weight of 61,000 (20). Their structures have not been determined but it is known that isocitrate lyase is a homotetramer (30).

A second malate synthase, malate synthase G (G since it is induced by glycolate) is also found in *E. coli*. This is encoded by *glcB*, and allows growth on glycolate or glyoxylate as a sole carbon source (21). The two malate synthases are regulated by distinct mechanisms and have different stabilities and inhibitory patterns (24).

Isocitrate dehydrogenase

Isocitrate dehydrogenase (IDH) is an enzyme of the TCA cycle that catalyzes the oxidative decarboxylation of isocitrate to α-ketoglutarate. IDH activity is regulated post-transcriptionally by phosphorylation, and this determines the flow of isocitrate either through the glyoxylate shunt or TCA cycle (44). Most bacteria have an $NADP^+$-linked IDH. Bacteria that have NAD^+-linked IDHs cannot grow on acetate, and lack either a respiratory chain or a complete TCA cycle (24). For bacteria capable of growing on acetate, the main source of NADPH required for biosynthesis (ca. 90%) comes from $NADP^+$-dependent enzymes (24). The *S. meliloti* NADP-IDH is a monomeric enzyme (78). The *E. coli* IDH is made up of two identical subunits, with a total molecular weight of 46,000 Da (109). Glyoxylate and oxaloacetate competitively inhibit the enzyme. It has been observed that the specific activity of IDH decreases as nitrogenase activity increases during *B. japonicum* symbiosis (47). This may be because under low oxygen conditions, the TCA cycle enzymes do not function very well.

A bifunctional enzyme IDH kinase/phosphatase catalyzes the phosphorylation and dephosphorylation of IDH. This regulatory enzyme is encoded by *aceK* (66). IDH kinase/phosphatase is a 67,000 Da homodimeric protein (22). The activity of this enzyme controls the carbon flux between the TCA cycle and the glyoxylate bypass. The reversible phosphorylation of IDH, a response to the external environment, also allows the bacteria to adapt to different intracellular conditions. In addition to kinase and phosphatase activities, the enzyme in *E. coli* also has ATPase activity (104). It has been established that one active site catalyzes the kinase/phosphatase reaction (55).

K_m and V_{max} Values at the Branch Point

A combination of *in vivo* and *in vitro* studies were used to characterize the branch point between the TCA cycle and glyoxylate shunt in *E. coli* (114). This study monitored the net flow of carbon through the major steps in acetate metabolism. The rates were determined by ^{13}C nuclear magnetic resonance spectroscopy, which looked at intracellular glutamate and measured rates of substrate incorporation into end-products. A series of conservation equations that described flux relationships of the system at a steady state were used to interpret the results. The results correlated well with kinetic studies,

substrate concentration and enzyme assays. At the branch point, isocitrate lyase and IDH compete for isocitrate. The rate at which radioactive acetate was incorporated through IDH was 2.6 times the rate through isocitrate lyase (V_{IDH}/V_{IL}=2.6). Another study showed that IDH has a much higher affinity for isocitrate than isocitrate lyase (K_m value of 8 mM compared to 600 mM) (68). In *B. japonicum* the isocitrate lyase and IDH K_m differ by only four-fold (62 μm and 16 μm respectively) (47) and this may allow enough isocitrate to pass through the glyoxylate shunt even if the IDH is not inhibited.

The Acetate Operon

It is now confirmed that in *E. coli*, the three genes coding for isocitrate lyase (*aceA*), malate synthase (*aceB*) and IDH kinase/phosphatase (*aceK*) are organized in an operon in the order *aceB-aceA-aceK* (Figure 1.3) (20). The order of genes was determined by deletion mapping. Precise mapping has placed the operon at 90.85 min. on the *E. coli* K-12 linkage map. The direction of transcription is from *aceB* to *aceA* (74). *aceA*::Tn*10* insertions eliminated only isocitrate lyase expression but *aceB*::Tn*10* eliminated expression of both enzymes.

S1 nuclease and deletion analysis indicates that a single promoter expresses the glyoxylate shunt when grown on acetate (20) (F. The promoter is found upstream from *aceB*. Although the genes of the *aceBAK* operon are expressed from a single promoter, the three enzymes are expressed at different rates (0.3: 1: 0.003). This may reflect the fact that the enzymes produced play different roles in the functioning of the glyoxylate bypass (25). How is differential expression achieved? Different codon usage, repetitive extragenic palindromic (REP) elements found in the intergenic regions between *aceA* and *aceK*, rapid degradation of the mRNA downstream region by 3' exonucleases, and premature transcriptional termination within the *aceK* are some of the reasons that have been suggested. This polarity has been observed in other operons too. The sequences responsible for inefficient expression of *aceK* are located in its ribosome binding site (20).

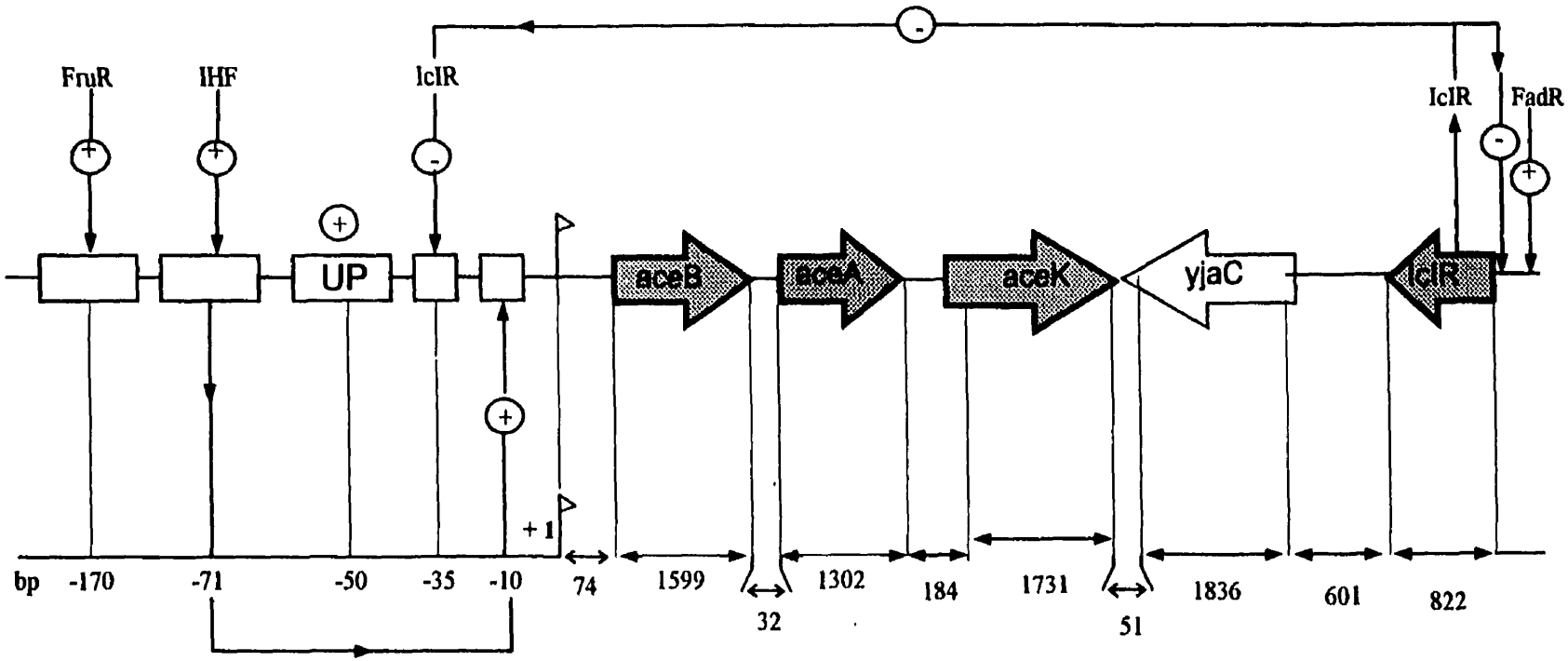

Figure 1.3. Organization of the *aceBAK* operon and the regulatory elements (not drawn to scale). The arrows show the direction of transcription of the genes. *+1* is the site of initiation of transcription. Negative and positive numbers denote the regions upstream or downstream from the initiation site respectively. *yjaC* separates *iclR* and *aceK* and may interfere with glyoxylate shunt enzyme activities. UP or upstream module is a promoter of *aceBAK*. The + or - signs suggest the type of regulation exerted on operon expression. FadR represses the *aceBAK* operon expression by stimulating (+) the expression of *iclR* (24). Numbers indicate the location and length of the various genes and elements in base pairs (from (24)).

Regulation of the Glyoxylate Shunt

The expression of the glyoxylate shunt enzymes in *E. coli* is induced during growth on acetate or fatty acids and repressed on a carbon source like glucose, pyruvate or glycerol (64). Isocitrate lyase in *B. japonicum* and *S. meliloti* is induced by acetate and oleate (60). IclR, FadR, integration host factor (IHF) and IDH (Figure 1.3) regulate the glyoxylate shunt at the level of transcription during growth on acetate. The different factors (Upstream module UP, IHF, FruR) that stimulate *aceBAK* induce conformational changes in DNA that show that the functioning of this operon strongly depends on the structural organization of the DNA matrix.

Effect of Metabolites and Growth Conditions on the Expression of the *ace* Operon

The glyoxylate shunt enzymes are not directly induced by acetate or acetyl-CoA (72). The *ace* operon is repressed, even in the presence of acetate, if a preferred carbon source like pyruvate or glucose is present (63). However, the rate of conversion of acetate to acetyl-CoA in these cases is the same. So what is the real inducer of *ace* operon transcription? One metabolite suggested is phosphoenolpyruvate (PEP). The complex that is formed between IclR and the operator/promoter region of *aceBAK* is insensitive to acetate, acetyl-CoA, acetyl phosphate, pyruvate, and oxaloacetate, but is critically impaired by PEP (23).

Other metabolites suggested are fructose-1-phosphate or fructose-1,6-bisphosphate (89, 90). When studying the binding capacity of FruR to various operons, these two molecules have been shown to displace the protein from the DNA even at low concentrations. Thus, in the presence of one of these molecules, operons like *aceBAK* that are under positive FruR control are not activated.

The glyoxylate shunt is repressed under anaerobic conditions. This repression is caused by the products of *arcA* and *arcB* (58), which also exert their activity over many other enzymes of aerobic pathways. Genetic analysis suggests that the genes compose a two-component regulatory system where *arcB* regulates *arcA* by phosphorylation (57).

arcA exhibits a 40% similarity to the *ompR* gene and has therefore been suggested to encode a DNA binding protein.

Expression of isocitrate lyase of *E. coli* is the same with glucose, pyruvate or glycerol as sole carbon source suggesting that the glyoxylate shunt operon is not subject to catabolite repression (107).

Glyoxylate Shunt Studies in Other Microorganisms

The organization and regulation of the glyoxylate bypass operon in other microorganisms has shown similarities, and some interesting differences, when compared with *E. coli*. In *S. typhimurium* LT2, the *aceBA* operon is induced by acetate to a level four times higher than in *E. coli* (118). As in *E. coli*, two malate synthase activities have been observed in *Rhizopus nigricans* (116). Two forms of isocitrate lyase have been observed in *Chlorella vulgaris* (50) and *Neurospora crassa* (98), but only one form is induced during growth on acetate. In *Yersinia pestis*, two forms of isocitrate lyase are seen during growth on acetate (52). One form, A, was present during growth on acetate but absent on carbon sources like glucose. The second form, B, was not constitutive but was found during growth on acetate and other carbon sources. In *Methylobacterium extorquens*, another bacterium with no isocitrate lyase, it is known that the genes *adhA* (alcohol dehydrogenase gene) and *meaA* (CoB_{12}-dependent mutase gene) are involved in an alternate pathway to the glyoxylate cycle (19). In an article by Han and Reynolds (49) three pathways for the oxidation of acetyl-CoA to glyoxylate have been proposed. There is no data, however, to suggest that any of these pathways actually occur. The IDH proteins in *Corynebacterium glutamicum* (35) and *Rhodomicrobium vannielii* (70) are monomeric. *Vibrio* sp. strain ABE-1 contains both a homodimeric and monomeric IDH (56).

There has been a report of *E. coli aceK* mutants capable of growing on acetate due to second-site mutations (67). Interestingly, these mutations did not map to any of the genes that encode glyoxylate shunt enzymes. This suggests that an alternative pathway may be present. Holms (54) suggested that glyoxylate could be oxidized in a cyclical manner, involving malate synthase, malic enzyme and pyruvate dehydrogenase.

Acetate Metabolism in *S. meliloti*

Acetate metabolism has been poorly addressed in *S. meliloti*, even though gluconeogenesis and TCA cycle intermediates like succinate have been extensively studied. In gluconeogenesis, glyceraldehyde-3-phosphate is synthesized from oxaloacetate via the enzymes phosphoenolpyruvate carboxykinase, enolase, phosphoglycerate kinase, and glyceraldehyde-3-phosphate dehydrogenase (40). Mutations in the genes encoding any of the above enzymes do not allow growth on either acetate or succinate. The *pckA* gene, encoding phosphoenolpyruvate carboxykinase, has been well characterized in *S. meliloti*. Expression of *pckA* is induced by gluconeogenic substrates (succinate, arabinose) but repressed by glucose (84).

Some TCA cycle enzymes such as citrate synthase, succinate dehydrogenase, α-ketoglutarate dehydrogenase, and isocitrate dehydrogenase have been studied in *S. meliloti* (33, 43, 61, 78). Malate dehydrogenase mutants are currently being investigated. Expression levels of TCA cycle enzymes depend on oxygen levels and carbon source in *E. coli* (25). Even though these two factors probably limit the functioning of this pathway in the bacteroids, various studies support the importance of a complete TCA cycle in both free-living and bacteroid forms. All of the TCA cycle mutants studied so far form ineffective nodules (34). Knowing the growth phenotype of mutants on various carbon sources can help in their characterization. Mutants defective in succinate dehydrogenase are unable to grow on acetate or succinate but grow well on malate or fumarate (43). Mutants defective in α-ketoglutarate dehydrogenase exhibit no growth on acetate, pyruvate and arabinose as sole carbon sources (33). Citrate synthase mutants are glutamate auxotrophs (34).

A study of two-carbon metabolism was initiated in our laboratory (108). Using Tn*5* mutagenesis, fifteen mutants of *S. meliloti* unable to utilize acetate as a sole source of carbon (Ace$^-$) were isolated. Complementing clones were isolated from the cosmid library of *S. meliloti* for six mutants. One acetate mutation (*ace13*) was found to be in the gene encoding pyruvate orthophosphate dikinase (PPDK). The PPDK protein catalyzes the reversible reaction

pyruvate + ATP + Pi ↔ PEP + AMP + PPi

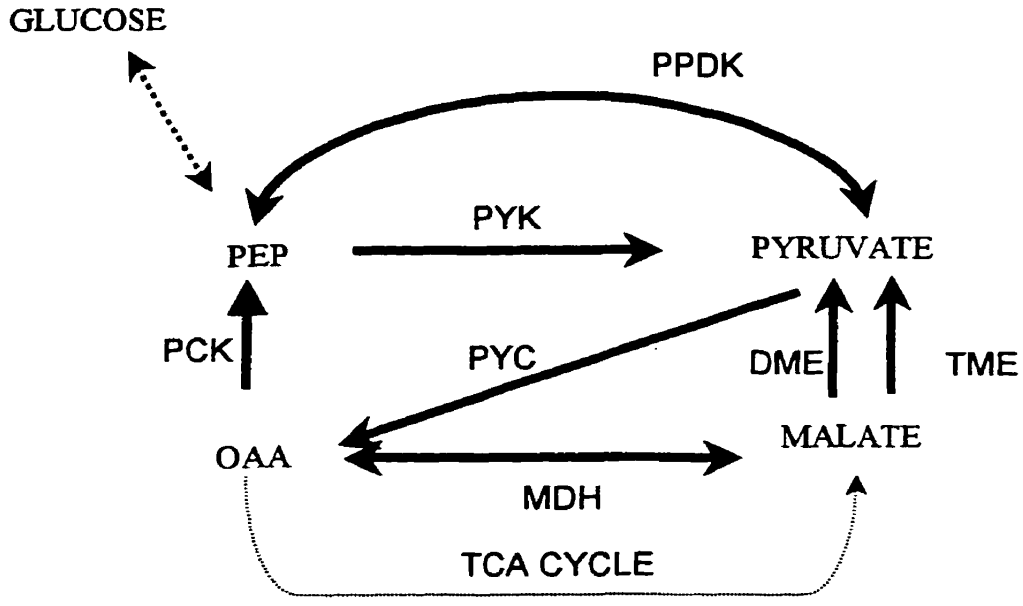

The formation of PEP is an important step in the gluconeogenic pathway in which TCA cycle intermediates can be converted to hexose sugars. The combined activities of malic enzyme and PPDK constitute a gluconeogenic pathway independent of PCK. Interestingly, the isolation of a *pod* mutant with an Ace^+ phenotype has been reported (82). The role of this enzyme may be in mediating PEP concentration, and this may be implicated in the PEP-dependent regulation of the *ace* operon by IclR.

This Work

Nodules and bacteria extracted from nodules usually contain relatively large amounts of short chain fatty acids, which can be metabolized through acetyl-CoA (2). In addition, our laboratory has been studying the degradation of poly-3-hydroxybutyrate (PHB) (17). Degradation of this polymer yields acetyl-CoA. The acetyl-CoA from PHB degradation would be expected to be converted to C_4-dicarboxylic acids via the glyoxylate shunt, but this has not been shown. We feel that a study of two-carbon metabolism will improve our knowledge of intermediary metabolism, and help us to better understand the various reactions that take place in the bacterium.

The objective of this project was to characterize the *S. meliloti* acetate utilization mutants isolated in our laboratory. A great deal of study has been done with *S. meliloti* because it has a well-developed genetic system. We also hoped to identify loci distinct to ones previously shown to be involved in acetate metabolism. Genes encoding glyoxylate shunt enzymes were of primary interest to us. The strategy was to:

- Isolate complementing clones for the remaining acetate mutants
- Map the *ace* mutations to the genome
- Obtain nucleotide sequences and thereby identify these genes
- Confirm the phenotype of mutants by biochemical analysis.
- Study the phenotype of the two *pod* mutants previously isolated.

CHAPTER 2

MATERIALS AND METHODS

MATERIALS AND METHODS

Bacterial Strains, Plasmids and Transposons

Bacterial strains, plasmids, transposons and phage used in this study are shown in Table 2.1. All strains used were from the laboratory collection. Bacterial strains were stored as frozen stocks at –70°C in LB containing 7% dimethylsulfoxide (DMSO). This minimized any spontaneous genetic alterations that would occur during long term storage.

Media, Antibiotics and Growth Conditions

All media used for growth of bacterial cultures was sterilized by autoclaving at 15 pounds/inch^2 at 121°C for 15 min. Bacterial strains were grown in either Tryptone Yeast (TY) (9) or Luria-Bertani (LB) (5) media. TY broth contained (g/l): Tryptone, 5; Yeast extract, 3; $CaCl_2.2H_20$, 4. LB broth contained (g/l): Tryptone, 10; Yeast extract, 5; NaCl, 10. Media was solidified with 1.5% Bacto-agar (Difco Laboratories, Detroit MI) in plastic petri dishes (95 x 15 mm, Fisher Scientific CO., Ottawa, Ont.). The minimal medium used was M9 salts (80). A 20 X M9 stock solution contained (g/l): Na_2HPO_4, 5.8; KH_2PO_4, 3; NaCl, 0.05 and NH_4Cl, 1.0. This medium was supplemented with 0.25 mM $CaCl_2$, 1 mM $MgSO_4$, 0.3 mg of biotin/l and the appropriate carbon source after autoclaving. The carbon source was usually used at a 15 mM concentration unless otherwise indicated. The amino acids isoleucine and valine (used in one growth experiment) were added at concentrations of 20 and 17 μg/ml respectively. Transductants were selected on LBM9 media (with neomycin or gentamicin-spectinomycin selection) to reduce phage nibbling. Antibiotics were used at the following concentrations (μg/ml): Neomycin (Nm), 200; Streptomycin (Sm), 200; Gentamicin (Gm), 20 (5 for *E. coli*); Spectinomycin (Sp), 100; Rifampicin (Rf), 50, Kanamycin (Km), 20; Tetracycline (Tc), 10; Chloramphenicol (Cm), 25; Ampicillin (Ap), 100. Antibiotics and amino acids were sterilized by filtering through a 0.45 μm syringe filter (Acrodisc, Gelman Sciences).

Indicator plates for β-galactosidase expression contained X-gal (5-bromo-4-chloro-3-indolyl-β-D-galactoside) at a concentration of 40 μg/ml. When working with strains harbouring plasmids, the appropriate antibiotics were added to ensure plasmid maintenance. If such a culture was used in conjugation, it was always centrifuged and resuspended in saline (0.85% NaCl) first. *S. meliloti* and *Agrobacterium* strains were grown at 30°C. *E. coli* was grown at 37°C. Small volume overnight cultures for experiments were grown in 16 x 150 mm tubes in a Rollordrum (New Brunswick Scientific Co., Edison N. J.) or in a shaker (200 rpm).

Conjugation

Conjugation involves the direct transfer of DNA from one cell to another upon contact. In the following experiments, conjugation was mostly performed to transfer a plasmid from one strain to another. Usually the plasmid had an *oriT* (this is the site nicked to initiate rolling cell replication and DNA transfer) but no *tra* genes, which are needed for the actual transfer process. In this case a mobilizer strain MT616, providing the *tra* functions in *trans*, was used in a triparental mating. Equal volumes of donor, recipient and mobilizer (if needed) were spotted on LB medium and incubated overnight. The mating spots were then suspended in saline and plated on appropriate selective media.

Preparation of ΦM12 Transducing Lysates

0.01 ml of a ΦM12 phage stock was added to 5 ml of *S. meliloti* culture. This was then incubated at 30°C with shaking for about 8 hours or until there was clearing of the culture (due to lysis of cells). 0.04 ml of chloroform was added to kill any viable cells that remained. Tubes were incubated at room temperature for an hour, transferred to plastic screw-cap tubes and stored at 4°C.

ΦM12-Mediated Transduction

In generalized transduction, relatively large segments of a bacterial cell's genome are transferred to another cell by bacteriophage particles that have acquired cellular DNA segments. Lysates were prepared as described (38). Equal volumes of diluted lysate (1:50) and recipient were mixed. The mixture was allowed to stand in a centrifuge tube for 20 min. at room temperature to allow adsorption of phage particles to the bacterial cell surface. The tubes were subsequently centrifuged at 6K rpm (SM-24 rotor, Sorvall RC-5B Superspeed Centrifuge, DuPont Instruments) for 5 min. The pellet was washed in saline and spread on LBM9 plates with the antibiotics for selection. Cotransduction frequencies were converted to distance in kb using Wu's formula (119).

Isolation of Complementing Clones

In bacterial genetics, genes are often cloned by phenotypic complementation. A previously prepared Rm1021 pLAFR1 (Tc^r) cosmid library (42) was introduced into the mutant and selected for the wild-type phenotype. The plasmid DNA was then further analyzed and characterized. pLAFR1 is approximately 22 kb, confers Tc^r and contains a unique *Eco*R1 site. The clone bank of *S. meliloti* was constructed using a partial *Eco*R1 digest of Rm1021 genomic DNA (42). Recombinant plasmids that complemented acetate mutations were identified by introducing the library into the mutant by conjugation followed by selection on M9 acetate. To prove that the isolated plasmids do in fact complement the mutant phenotype, the plasmid was first transferred to *E. coli* MT607 and then back to the *S. meliloti* mutant. Both transfers were done by conjugation.

Transposon Replacements

It is useful to exchange a Tn*5* insertion for a Tn*5* derivative since sometimes a strain that is used in the experiment with the mutant could confer the same antibiotic resistance. We replaced the Tn*5* insertion by Tn*5*-233 (which confers Gm^r Sp^r) using previously described procedures (46). The method is based on the homologous recombination between the IS*50* elements, which is common to both transposons. pRK607 was mated from *E. coli* into the *S. meliloti* recipient (carrying the Tn*5* insertion). After selecting for Gm^r Sp^r transconjugants, colonies that had undergone true replacements were identified by screening for loss of Nm resistance.

Genetic Mapping

Mutations were mapped onto the chromosome in a way similar to Hfr mapping in *E. coli* (40). There are seven mapping strains, each having a Tn*5*-*mob* in a different position or orientation in the chromosome (62). The mutations were transduced into each of the seven mapping strains and then mobilized out of each strain into Rm5000 in a triparental mating. The frequency with which the mutation was transferred from each Tn*5*-*mob* insertion was then determined. The position of the mutation was between insertions from which it was transferred at the highest frequency.

Transposon Mutagenesis of Plasmids

The plasmid to be mutagenized (in this study the plasmids were the complementing clones) was first transferred to the *E. coli* strain MT614 by conjugation. This strain has a chromosomal Tn*5* insert. Transferring the plasmid into the original mutant (*ace*::Tn5-233, Gm^r Sp^r) and selecting for the Tn5 insertion identified transposition of the Tn5 onto the plasmid. Plasmids that were unable to complement the original mutant were then chosen. Position of the Tn*5* insertion on the plasmid was determined by restriction analysis of the plasmid DNA using the enzymes *Eco*RI, *Hin*dIII

and *Bam*HI. A few complementing clones were mutagenized with Tn*5*-B20, a Tn*5* derivative that has a promoterless reporter gene, *lacZ*. This would be useful for study of expression of these genes later on. The method was the same except that the transposon donor was G312, harbouring a chromosomal Tn*5*-B20 insert. In addition to the antibiotics for selection, the plates also contained X-gal. Plasmids that were unable to complement and gave blue colonies on X-gal plates were chosen for further study.

Homogenotization

Tn*5* insertions in the complementing clones were recombined into the homologous region of the *S. meliloti* genome (93) by introducing an incompatible plasmid. The recombinant pLAFR1 plasmid carrying the Tn*5* insertion in *S. meliloti* DNA was introduced into Rm1021 by conjugation. Then the incompatible plasmid pPH1JI was introduced into Rm1021 carrying the Tn*5* insertion plasmid, with selection for the transposon (Nm^r) and the incoming plasmid pPH1JI (Gm^r). Both pLAFR1 and pPH1JI belong to the IncP group of plasmids. Since only one plasmid of an incompatibility group can be stably maintained in a cell, Gm^r Nm^r transconjugants that arise will have lost the pLAFR1 (loss of Tc^r) but will have retained the transposon (Nm^r).

β-Galactosidase Assays

The β-galactosidase activity of *S. meliloti* was measured using o-nitrophenyl β-D-galactopyranoside (ONPG) as substrate, as described by Miller and modified by Stachel (80, 100). For kinetic analysis, 300 ml defined media in a 1 l Erlenmeyer Flask was inoculated with 1.5 ml of an overnight TY culture. The cultures were incubated with shaking, and samples (1.5 ml) were removed every 4 hours and promptly frozen. For the assay, the samples were thawed on ice. Culture sample was diluted with an equal volume of Z buffer (Z buffer contained per liter: 16.1 g $Na_2HPO_4.7H_20$, 5.5 g $NaH_2PO_4.H_20$, 0.75 g KCl, 0.246 g $MgSO_4.7H_2O$, 2.7 g β-mercaptoethanol). OD_{600} was measured. To 0.6 ml of diluted sample, 40 µl of 0.1% SDS and 40 µl chloroform was added to permeabilize

the cells. A brief vortex (10 seconds) and a 10-minute equilibration at room temperature followed this. 100 µl ONPG (4 mg/ml in Z buffer) was then added to start the reaction. The reaction was stopped with 1M Na_2CO_3 when a light yellow colour developed in the samples. Cells were pelleted and A_{420} of supernatant was measured. Miller units were calculated by using the formula

$$1 \text{ Miller Unit (U)} = (1000 * A_{420})/ (t * v * OD_{600})$$

Where t = time of incubation and v = volume of culture used in assay

A UV/Visible spectrophotometer (Ultrospec 2000, Pharmacia Biotech) was used for the measurements of optical density.

Preparation of Cell-Free Extracts

250 ml of desired media was inoculated with an overnight cell culture. The starter culture was washed with saline before inoculation if the second medium was a minimal medium. The cultures were incubated with shaking (200 rpm) in a 30°C incubator until the cells reached late log phase/early stationary phase. Cultures were checked for purity by streaking on TY plates. The cultures were transferred to 250 ml centrifuge bottles and centrifuged (GSA rotor, 5K, 20 min.). The cells were washed twice in a washing buffer (20 mM Tris-Cl, pH 7.8, 1 mM $MgCl_2$). The wet weight was determined and the pellets were stored at –20°C. The cells were resuspended in freshly prepared sonication buffer (20 mM Tris-Cl, pH 7.8, 1 mM $MgCl_2$, 10% glycerol, 10 mM β-mercaptoethanol) to reach a final concentration of 4 ml buffer/ g cells wet weight. Cells were disrupted by sonication (Ultrasonics Sonifier Cell Disruptor Model W185-D). Cells were sonicated in a plastic beaker on ice for 15-second pulses with periods of cooling in between. The microtip (sonicator probe) had a power output level of 7. Total sonication time was about 5 min. Well-sonicated extracts are usually clear and viscous. The extracts were then put into 15 ml plastic tubes and centrifuged (SS34 rotor, 10K, 30 min.). Supernatant was

transferred to a sterile centrifuge tube and 1 ml aliquots were transferred to eppendorf tubes. The tubes were stored at –70°C.

Protein concentration was determined by the Bradford method (11) using the BioRad protein assay dye (Coomassie blue). Bovine serum albumin was used as a standard.

Enzyme Assays

Isocitrate Lyase Activity

Isocitrate lyase activity was assayed according to the method described by Dixon and Kornberg (31). Strains were grown in TY medium supplemented with 10 mM glucose, and cell extracts were prepared as described. 50 µl cell free extract was added to a reaction mixture containing 0.1 M potassium phosphate, 1 M $MgCl_2$, 10 mM phenylhydrazine–HCl, 50 mM cysteine and 25 mM isocitrate in a total volume of 1.5 ml. Negative control was a mixture with no substrate (isocitrate). Isocitrate lyase catalyzes the reaction

$$\text{isocitrate} \longrightarrow \text{succinate} + \text{glyoxylate}$$

The rate of increase OD_{324} due to the formation of glyoxylic acid phenylhydrazone was measured. $\in_{324}$ for glyoxylic acid phenylhydrazone = 1.7×10^4. Values presented are the mean of three assays.

Malate Synthase Activity

Malate synthase was also assayed according to Dixon and Kornberg (31). Strains were grown in TY medium supplemented with 10 mM glucose and cell extracts were prepared as described. 50 µl of cell free extract was added to a reaction mixture containing 0.1 M Tris-HCl (pH 7.4), 1 M $MgCl_2$, acetyl-CoA (5 mg/ml) and 0.02 M glyoxylic acid in a total volume of 1.5 ml. Negative control had no substrate (acetyl-CoA). Malate synthase catalyzes the reaction

acetyl-CoA + glyoxylate ⟶ malate

The principle of this assay depends on measurement of rate of decrease of OD_{232} due to the breakage of the thio-ester bond of acetyl-CoA in the presence of glyoxylate. $\in_{232}$ for the cleavage of thio-ester bond of acetyl-CoA = 4.5×10^3 (101).

Acetyl-CoA Synthetase Activity

A coupled assay was used to detect the activity of acetyl-CoA synthetase (ACS) (12). Strains were grown to late log phase in 15 mM M9 minimal glucose and cell extracts were prepared as described. In *S. meliloti*, the highest activity of ACS has been observed in glucose medium (13). 20 µl of cell free extract was added to the assay mixture containing 100 mM Tris-HCl (pH 8.0), 5 mM $MgCl_2$, 5 mM NAD^+, 0.1 mM CoA, 5 mM L-malate, 10 mM potassium acetate, 12.5 µg/ml malate dehydrogenase and 25 µg/ml citrate synthase. The absorbance was measured for about one minute to determine the background activity (ATP-independent NADH reaction). The reaction was then initiated by the addition of 10 mM ATP. The reactions that occur in the assay tubes:

acetate + ATP + CoA ⟶ acetyl-CoA + AMP + PPi

malate + **NAD^+** ⟶ oxaloacetate + **NADH**

acetyl-CoA + oxaloacetate ⟶ citrate + CoA

The rate of NADH formation was monitored as an increase in absorbance at 340 nm. The background rate of NADH production present without ATP was subtracted from the rate measured in the assay to calculate enzyme activity. $\in_{340}$ for NADH = 6.22×10^3 M^{-1} cm^{-1}.

Acetoacetyl-Coenzyme A Synthetase Activity

The acetoacetyl-CoA synthetase assay was carried out the same way as the acetyl-CoA synthetase assay except that 10 mM potassium acetoacetate was used instead of 10 mM potassium acetate. In addition, the reaction mixture contained 50 mM KCl. The rate of NADH formation was once again monitored.

Growth Experiments

Overnight cultures of *S. meliloti* were grown to late log phase, washed once in saline and 0.1 ml subcultured into 5 ml M9, supplemented with the appropriate carbon source in a 16 mm X 150 mm culture tube, and placed in a shaker (200 rpm) or Rollordrum at 30°C. Growth was followed by measuring absorbance at 600 nm (Spectronic 20D+, Bausch and Lomb). The mean growth rate constant (k) is the rate of growth in a culture, and the reciprocal of k gives the mean generation time or doubling time (g) (88).

$$k = \log(A_2)-\log(A_1)/(.301)(t) \text{ and } g = 1/k$$

where k = mean growth constant (generations/hr)

g = mean generation time (hr/ generation)

A_1 = initial absorbance at time t_1

A_2 = absorbance at time t_2

At the end of the experiment, cultures were checked for purity by streaking on TY agar.

Growth Competition Assays

Overnight cultures of the two strains to be tested were diluted to an OD_{600} of 1.0 and 50 µl of each were inoculated into 5ml 15 mM M9 glucose. This ensured that the wild-type and mutant cultures were mixed in a ratio of 1:1. Tubes were placed in a shaker at 30°C for 5 min. 0.1 ml of the culture was removed for titration and the tubes were put

back at 30°C with shaking for 24 hours. 0.1 ml was removed for cfu titration and another 0.1 ml used to subculture 5 ml of 2.5 mM M9 glucose. The tubes were incubated for 24 hours at 30°C with shaking. Subcultures were repeated alternating between carbon-rich (15 mM M9 glucose) and carbon-poor (2.5 mM M9 glucose) media, doing a cfu titration at each subculture. The phenotype of the representative colonies that arose on cfu plates was scored. The two strains alone were used as controls.

DNA Manipulations

Standard protocols were used for the manipulation of DNA (6, 95). Restriction enzymes and T4 DNA ligase (Boehringer Manheim or GIBCO/BRL) were used as recommended using the supplied buffers. Agarose gel electrophoresis was carried out in a horizontal gel apparatus. 0.8% agarose (BioShop Canada) with 1X TAE buffer (0.04 M Tris-acetate and 0.002 M EDTA, pH 8.0) was used in the preparation of gels. DNA was visualized by staining the gel with ethidium bromide (10 mg/ml). The size of DNA fragments was estimated using standard markers – Lambda DNA cut with *Hin*dIII (GIBCO/BRL). Gel was placed on an UV illuminator and photographed with a Polaroid camera.

Plasmid Minipreps

Two methods were used to isolate plasmid DNA on a small scale from *E. coli*. For routine isolations, 1.5 ml of an overnight *E. coli* culture (LB medium plus any antibiotics required) was centrifuged for one minute in an Eppendorf tube. The pellet was suspended in 0.1 ml TEG buffer (50 mM Tris-Cl, 20 mM EDTA, 1% glucose, pH 8.0) containing ribonuclease (200 μg/ml). 0.2 ml alkaline lysing solution (ALS; 0.2 M NaOH, 1% SDS) and 0.15 ml sodium acetate (pH 4.8) were then added and the tubes were cooled on ice for 2 min. The samples were then centrifuged for 5 min. To the supernatant, 0.9 ml of 95% ethanol was added. This step precipitates the DNA. A final ethanol wash (70% ethanol) solubilized the salts in the pellet. The pellet was then allowed to dry

completely before suspending it in TE buffer (10 mM Tris-Cl, 1 mM EDTA, pH 8.0). The buffer volume usually depended on whether the plasmid being isolated was a low-copy or high-copy number vector. The samples were then incubated at 65°C for 15 min. to dissolve DNA and stored at –20°C.

The second method was used for the purpose of sequencing and gave cleaner DNA. A 5 ml culture was grown to late log phase. Cells were pelleted out. 0.1 ml TEG buffer with ribonuclease and 0.2 ml ALS were added and the tubes were mixed well. After the addition of 0.15 ml 7.5 M ammonium acetate, the tubes were centrifuged for 10 min. in a bench top centrifuge (IEC Micromax). Supernatant was transferred to a fresh microfuge tube. 0.3 ml isopropanol was added to precipitate the DNA and the samples were centrifuged for 10 min. To the pellet, 0.075 ml 7.5 M ammonium acetate and 0.2 ml TE buffer were added. After a brief vortex, samples were kept on ice for 15 min. before centrifuging for 10 min. To the supernatant, 0.275 ml isopropanol was added and DNA was collected by centrifugation for 15 min. The pellet was washed in 70% ethanol and dried completely. DNA was resuspended in TE buffer.

Subcloning and *E. coli* Transformation

Vector and fragment to be subcloned were prepared by digesting with restriction enzymes. Heating the samples at 65°C for 5 min. inactivated the restriction enzymes. Linearized vector plasmid DNA and a three to ten-fold molar excess of the fragment to be subcloned were mixed together. Total volume for ligation was usually 20 µl. Ligation was usually carried out at room temperature for 30 min. or at 15°C in a thermocycler (PTC-100 Programmable Thermal Controller, MJ- Research, Inc.) overnight. This DNA was used to transform competent *E. coli* DH5α cells. Cells were made competent according to the calcium-glycerol method (7). To the ligation mixture, 0.1 ml competent cells and ice-cold 100 mM $CaCl_2$ were added, mixed very carefully with pipette tip and kept on ice for 30 min. Tubes were incubated for 90 seconds at 42°C (heat shock) then immediately transferred to ice for 2 min. 0.5 ml LB was added to the mixture and tubes were incubated at 37°C for 30 min. This step allowed the expression of plasmid encoded

antibiotic resistance. The cells were then pelleted, resuspended in 120 µl LB, and 100 µl, 10 µl and 1 µl aliquots were removed and plated on LB with the appropriate antibiotics.

DNA Sequencing and Analysis

DNA was sequenced using automated sequencing (MOBIX Facility, McMaster University). The primer used in gene sequencing was specific to the IS*50* element. The oligonucleotide primer sequence is 5'-GCC CAG TCG GCC GCA CGA TGA AGA GCA-3' (18). Tn*5*-B20 has only one intact IS50 site. The other site is partly deleted and disrupted by the *lacZ* gene. Therefore the Tn*5*-B20 mutagenized clones could be sequenced directly. Since these plasmids were relatively large (ca. 40 kb), the region flanking *ace*::Tn*5*-B20 was subcloned from the transposon mutagenized plasmid as a Km^r *Eco*RI fragment. Nucleotide and amino acid sequences were compared to GenBank using BLAST software (1, 45).

Table 2.1. Bacterial strains, plasmids and phage used in this study.

Strain, plasmid, transposon or phage	Relevant characteristics	Source, reference or construction
Strains		
S. meliloti		
Rm1021	SU47 *str-21*	(79)
Rm5000	SU47 *rif-5*	(38)
Rm5439	Rm1021, *pckA1*::Tn*V*	(40)
Rm8501	Rm1021, Lac$^-$	(46)
Rm11106	Rm1021, *ace1*::Tn*5* (group I)	Lab Collection
Rm11132	Rm1021, *ace2*::Tn*5*	Lab Collection
Rm11134	Rm1021, *acsA7*::Tn5	(14)
Rm11137	Rm1021, *ace3*::Tn*5*	Lab Collection
Rm11141	Rm1021, *ace4*::Tn*5* (group I)	Lab Collection
Rm11199	Rm1021, *ace10*::Tn*5*	(108)
Rm11200	Rm1021, *ace13*::Tn*5* (group II; *pod*)	(108)
Rm11201	Rm1021, *ace18*::Tn*5*	(108)
Rm11239	Rm1021, *ace1*::Tn*5*-233 (group I)	Tn*5*-233 replacement of Rm11106
Rm11240	Rm1021, *ace2*::Tn*5*-233	Tn*5*-233 replacement of Rm11132
Rm11241	Rm1021, *ace3*::Tn*5*-233	Tn*5*-233 replacement of Rm11137
Rm11242	Rm1021, *ace4*::Tn*5*-233 (group I)	Tn*5*-233 replacement of Rm11141
Rm11243	Rm1021, *ace10*::Tn*5*-233	Tn*5*-233 replacement of Rm11199
Rm11244	Rm1021, *ace13*::Tn*5*-233 (group II; *pod*)	Tn*5*-233 replacement of Rm11200
Rm11245	Rm1021, *ace18*::Tn*5*-233	Tn*5*-233 replacement of Rm11201
Rm11314	Rm1021, *pod14*::Tn*5*	Homogenote of pZT14
Rm11327	Rm1021, *pod*::Tn5, Ace$^-$	ΦRmG274 ----- > Rm1021
Rm11328	Rm1021, *pod*::Tn5, Ace$^-$	ΦRmG274 ----- > Rm1021
Rm11338	Rm1021, *pod*::Tn5, Ace$^+$	ΦRmG274 ----- > Rm1021
Rm11339	Rm1021, *pod*::Tn5, Ace$^+$	ΦRmG274 ----- > Rm1021
Rm11358	Rm8501, *pod15*::Tn*5*-B20	This study
Rm11364	Rm1021, *acsA7*::Tn*5*, *ace15*::Tn*5*-233	ΦRm11134 ------ > Rm11388
Rm11374	Rm1021, *ace5*::Tn*5* (group IV; *hemN*)	Lab Collection
Rm11375	Rm1021, *ace6*::Tn*5* (group IV)	Lab Collection
Rm11376	Rm1021, *ace7*::Tn*5* (group III)	Lab Collection
Rm11377	Rm1021, *ace8*::Tn*5* (group IV)	Lab Collection
Rm11378	Rm1021, *ace9*::Tn*5*	Lab Collection

Rm11379	Rm1021, *ace11*::Tn*5*	Lab Collection
Rm11380	Rm1021, *ace12*::Tn5	Lab Collection
Rm11381	Rm1021, *ace14*::Tn5 (group IV)	Lab Collection
Rm11382	Rm1021, *ace15*::Tn5 (group III; *acsB*)	Lab Collection
Rm11383	Rm1021, *ace5*::Tn*5*-233 (group IV; *hemN*)	Tn*5*-233 replacement of Rm11374
Rm11384	Rm1021, *ace8*::Tn*5*-233 (group IV)	Tn*5*-233 replacement of Rm11377
Rm11385	Rm1021, *ace9*::Tn*5*-233	Tn*5*-233 replacement of Rm11378
Rm11386	Rm1021, *ace11*::Tn*5*-233	Tn*5*-233 replacement of Rm11379
Rm11387	Rm1021, *ace14*::Tn*5*-233 (group IV)	Tn*5*-233 replacement of Rm11381
Rm11388	Rm1021, *ace15*::Tn*5*-233 (group III; *acsB*)	Tn*5*-233 replacement of Rm11382
RmG274	Rm1021, *pod-5*::Tn*5*	(82)
RmG139	Rm1021, *pod-1*	(82)
RmH347	Ω601::Tn*5*-*mob* (-)	(37, 62)
RmH348	Ω602::Tn*5*-*mob* (+)	(37, 62)
RmH349	Ω611::Tn*5*-*mob* (+)	(37, 62)
RmH350	Ω612::Tn*5*-*mob* (-)	(37, 62)
RmH351	Ω614::Tn*5*-*mob* (+)	(37, 62)
RmH352	Ω615::Tn*5*-*mob* (-)	(37, 62)
RmH353	Ω637::Tn*5*-*mob* (+)	(37, 62)
***Escherichia coli* derivatives**		
DH5α	F⁻ *endA1 hsdR17* (rk^-, mk^-) *supE44 thi-1 recA1 gyrA96 relA1* Δ(*argF-lacZYA*)U169 Φ80d*lacZ* ΔM15, λ^-	GIBCO BRL
G312	MT607Ω5::Tn*5*-B20	(32)
MT607	*pro-82, thi-1, endA, hsdR17 supE44, recA56*	(39)
MT614	MT607ΩTn*5*	(122)
MT616	MT607(pRK600); mobilizer	(39)
Plasmids		
pGQ105	pSP329 carrying the *S. meliloti acsA* gene on a 4.0 kb *Kpn*I fragment	G. -Q. Cai
pENO	pLAFR1, complements enolase mutants	
pPGK/GAP	pLAFR1, complements 3-phosphoglycerate kinase and glyceraldehyde-3-phosphate dehydrogenase mutants	

pPCK	pLAFR1, complements phosphoenolpyruvate carboxykinase mutants	
pPH1JI	Gm^r, Sp^r, Cm^r IncP plasmid	(10)
pLAFR1	IncP cosmid cloning vector, Tc^r	(42)
pUC18	ColE1 cloning vector, Ap^r	(121)
pRK607	pRK2013::Tn*5*-233; Nm-Km^r, Gm^r, Sp^r	(28)
pRK600	pRK2013 *npt*::Tn*9* Cm^r	(39)
pTC197	ColE1 cloning vector, Gm^r	T. C. Charles
pZT1	pLAFR1 clone, complements Rm11106 (group I mutant)	(108)
pZT2	pLAFR1 clone, complements Rm11106 (group I mutant)	(108)
pZT3	pLAFR1 clone, complements Rm11132	(108)
pZT4	pLAFR1 clone, complements Rm11132	(108)
pZT5	pLAFR1 clone, complements Rm11137	(108)
pZT6	pLAFR1 clone, complements Rm11137	(108)
pZT7	pLAFR1 clone, complements Rm11137	(108)
pZT8	pLAFR1 clone, complements Rm11141 (group I mutant)	(108)
pZT9	pLAFR1 clone, complements Rm11200 (*pod* mutant)	(108)
pZT10	pLAFR1 clone, complements Rm11200 (*pod* mutant)	(108)
pZT11	pLAFR1 clone, complements Rm11200 (*pod* mutant)	(108)
pZT12	pLAFR1 clone, complements Rm11201	(108)
pZT13	pLAFR1 clone, complements Rm11201	(108)
pZT14	pZT9ΩTn*5*, Nm^r	(108)
pZT15	pTC197 carrying a Km^r *Bam*HI fragment of pZT9ΩTn*5*	(108)
pZT16	pTC197 carrying Km^r *Bam*HI fragment of pZT9ΩTn*5*	(108)
pZT17	pLAFR1 clone, complements Rm11376 (group III mutant)	This study
pZT18	pLAFR1 clone, complements Rm11379	This study
pZT19	pLAFR1 clone, complements Rm11379	This study
pZT20	pLAFR1 clone, complements Rm11379	This study
pZT21	pLAFR1 clone, complements Rm11379	This study
pZT22	pLAFR1 clone, complements Rm11380	This study
pZT23	pLAFR1 clone, complements Rm11380	This study
pZT24	pLAFR1 clone, complements Rm11381 (group IV mutant)	This study
pZT25	pLAFR1 clone, complements Rm11381 (group IV mutant)	This study
pZT26	pLAFR1 clone, complements Rm11382 (*acsB* mutant)	This study

pZT27	pLAFR1 clone, complements Rm11382 (*acsB* mutant)	This study
pZT28	pLAFR1 clone, complements Rm11382 (*acsB* mutant)	This study
pZT29	pLAFR1 clone, complements Rm11374 (*hemN* mutant)	This study
pZT30	pLAFR1 clone, complements Rm11374 (*hemN* mutant)	This study
pZT31	pLAFR1 clone, complements Rm11374 (*hemN* mutant)	This study
pZT32	pLAFR1 clone, complements Rm11375 (group IV mutant)	This study
pZT33	pLAFR1 clone, complements Rm11376 (group IV mutant)	This study
pZT34	pLAFR1 clone, complements Rm11376 (group IV mutant)	This study
pZT35	pLAFR1 clone, complements Rm11377 (group IV mutant)	This study
pZT36	pLAFR1 clone, complements Rm11377 (group IV mutant)	This study
pZT37	pLAFR1 clone, complements Rm11377 (group IV mutant)	This study
pZT38	pUC18 carrying Km^r *Eco*R1 fragment from pZT42	This study
pZT39	pUC18 carrying Km^r *Eco*R1 fragment from pZT47	This study
pZT40	pZT9ΩTn*5*-B20, Nm^r	This study
pZT41	pZT31ΩTn*5*-B20, Nm^r	This study
pZT42	pZT31ΩTn*5*-B20, Nm^r	This study
pZT43	pZT24ΩTn*5*-B20, Nm^r	This study
pZT44	pZT24ΩTn*5*-B20, Nm^r	This study
pZT45	pZT24ΩTn*5*-B20, Nm^r	This study
pZT46	pZT26ΩTn*5*-B20, Nm^r	This study
pZT47	pZT26ΩTn*5*-B20, Nm^r	This study
pZT48	pUC18 carrying Km^r *Eco*R1 fragment from pZT45	This study
Transposons		
Tn*5*	Nm^r, Sm^r (pRK602)	(8)
Tn*5*-233	Gm^r-Sp^r (pRK607)	(28)
Tn*5*-B20	Tn*5* derivative generating *lacZ* transcriptional fusion, Nm^r	(97)
Tn*5*-11	*oriT* of pRK2 cloned into Tn*5*-233, Gm^r-Sp^r (pTFM1)	(39)
Phage		
ΦM12	*S. meliloti* transducing phage	(38)

CHAPTER 3
RESULTS

RESULTS

The objective of this study was to characterize acetate mutations in loci not previously described. Since the operation of the glyoxylate shunt is required by many organisms for the metabolism of acetate, we expected to find mutations in the genes encoding isocitrate lyase and malate synthase. Mutations that affect gluconeogenesis (40) and TCA cycle enzymes like α-ketoglutarate dehydrogenase and succinate dehydrogenase (33, 43) have also been shown to cause an acetate minus phenotype in *S. meliloti*. However, examining the growth phenotype of mutants on various carbon sources can allow identification of these mutations. Fifteen catabolic mutants that were defective in acetate metabolism were identified previously in our lab (108). The mutants were termed Ace for "Acetate utilization". These mutants had been screened for their inability to grow on acetate minimal medium, while retaining the ability to grow on glucose minimal medium. Cotransduction experiments confirmed that the phenotypes were due to the Tn*5* insertion in each case.

Identification of Mutants in Previously Studied Genes

The first step was to identify mutants with defects in known functions. The mutants were grown on different carbon sources and checked for complementation by gluconeogenic clones (Tables 3.1 and 3.2). These clones had been isolated in a previous study (40). Strains having mutations in the genes encoding gluconeogenesis or TCA cycle enzymes have an Ace$^-$ phenotype. Gluconeogenic mutants also do not grow on succinate (40). Mutations in genes encoding the TCA cycle enzymes succinate dehydrogenase and α-ketoglutarate dehydrogenase will not allow growth on arabinose (33). Seven Ace mutants were affected in growth on succinate and arabinose (Table 3.1).

Table 3.1. Growth[a] of *S. meliloti* acetate utilization mutants on minimal medium containing different carbon sources

Allele	Carbon source*					
	GLU	ACE	SUCC	ARA	AA	3-HB
ace1	++	+/-	++	++	+/-	+
ace2	+	+/-	+	+	-	+/-
ace3	++	-	-	+/-	+/-	+
ace4	++	+/-	++	++	+/-	+
ace5	++	-	++	++	+/-	+/-
ace6	++	-	-	+/-	-	-
ace7	++	-	++	++	++	++
ace8	++	-	++	++	+/-	+/-
ace9	++	-	-	-	+/-	+/-
ace10	+	+/-	-	+/-	+/-	+
ace11	++	-	-	-	+/-	+/-
ace12	++	-	-	-	+/-	+
ace13	++	-	++	++	-	+/-
ace14	++	-	++	++	+/-	+/-
ace 15	++	-	++	++	++	++

*All plates had a carbon source concentration of 15 mM. GLU, Glucose; ACE, Acetate; SUCC, Succinate; ARA, Arabinose; AA, Acetoacetate; 3-HB, 3-hydroxybutyrate.

[a]Symbols: ++, Growth as well as the wild type; +, Less growth than the wild type; +/-, Leaky growth; -, No growth.

Since gluconeogenic mutants have already been described (40), and corresponding complementing clones were available, we decided to determine whether the succinate and arabinose utilization mutants were indeed deficient in gluconeogenic enzymes. We could then put them aside, and continue characterization of the rest. The gluconeogenic clones encoded the enzymes phosphoenolpyruvate carboxykinase (Pck),

3-phosphoglycerate kinase (Pgk), glyceraldehyde-3-phosphate dehydrogenase (Gap) and enolase (Eno) (40). The gluconeogenic clones were transferred to the mutants and checked for phenotypic complementation (Table 3.2). Six mutants were thus identified as gluconeogenic mutants whilst the *ace6* mutant was not complemented by the gluconeogenic clones.

Table 3.2. Complementation with gluconeogenic clones for growth on acetate minimal media

Allele	**Plasmid***		
	pPCK	**pPGK/GAP**	**pENO**
ace1	-	-	-
ace2	+	-	-
ace3	-	+	-
ace4	-	-	-
ace5	-	-	-
ace6	-	-	-
ace7	-	-	-
ace8	-	-	-
ace9	-	-	+
ace10	-	+	+
ace11	-	-	+
ace12	-	+	-
ace13	-	-	-
ace14	-	-	-
ace15	-	-	-

*The plasmids encode the enzymes phosphoenolpyruvate carboxykinase (PCK), 3-phosphoglycerate kinase (PGK), glyceraldehyde-3-phosphate dehydrogenase (GAP) and enolase (ENO). The gluconeogenic clones were transferred to the mutants by conjugation and checked for phenotypic complementation on acetate. '+' indicates complementation by clones; '-'indicates no complementation.

Mutant Groups

The nine remaining mutants with no defects in known gluconeogenic enzymes were next put into groups by merodiploid complementation analysis and transductional linkage analysis. Recombinant plasmids, which complemented the individual mutations, were previously isolated for six of the mutants and were available in our laboratory collection (108). Complementing clones for the other mutants were isolated in this study. Approximately six complementing clones were isolated for each mutant. One representative clone for each was chosen for further study. The complementing plasmid from each mutant was introduced into each of the other mutants and checked for phenotypic complementation (see Table 3.3).

Table 3.3. Complementation of *ace* mutants with complementing clones from other mutants

Allele	**Mutant and recombinant plasmid***								
	(pZT2) *ace1*	(pZT8) *ace4*	(pZT31) *ace5*	(pZT32) *ace6*	(pZT17) *ace7*	(pZT36) *ace8*	(pZT9) *ace13*	(pZT25) *ace14*	(pZT27) *ace15*
ace1	+	-	-	-	-	-	-	-	-
ace4	+	+	-	-	-	-	-	-	-
ace5	-	-	+	-	-	+	-	-	-
ace6	-	-	-	+	-	-	-	-	-
ace7	-	-	-	-	+	-	-	-	+
ace8	-	-	-	-	-	+	-	-	-
ace13	-	-	-	-	-	-	+	-	-
ace14	-	-	-	-	-	+	-	+	-
ace15	-	-	-	-	+	-	-	-	+

*The complementing plasmid from each mutant was put into other mutants and checked for phenotypic complementation on acetate minimal media. '+' indicates complementation by complementing clone; '-' indicates no complementation.

Cotransduction experiments were performed between insertions to determine if they were linked (see Table 3.4). For example, in order to determine the linkage between *ace5* and *ace8*, a lysate of Rm11374 was used to transduce the insertion into strain Rm11384 (*ace8*ΩTn*5*-233). The transductants were screened for Gm^r Sp^r to see if the Tn*5* was cotransducible with Tn*5*-233. There is a relationship between cotransduction frequency and distance (119). If two insertions are 100% linked, they are at the same position or very close to each other. *ace1* and *ace4* were 80% linked. *ace7* and *ace15* were 100% linked. *ace13* was not linked to any of them. *ace5*, *ace6*, *ace8* and *ace14* were tightly linked (*ace5* was 100% linked to *ace8* and 93% linked to *ace14*; *ace6* was 100% linked to *ace8*; *ace8* was 100% linked to *ace14*). Based on these data, the mutations were placed into four groups:

Group I – *ace1*, *ace4*

Group II – *ace13*

Group III – *ace7*, *ace15*

Group IV – *ace5*, *ace6*, *ace8*, *ace14*

Table 3.4. Cotransduction linkage analysis of *ace* mutations (%)

		Donor (*ace* mutant)								
Recipient (Ace mutant)		1	4	5	6	7	8	13	14	15
	1	*								
	4	80	*							
	5	0	-	*						
	6	-	-	-	*					
	7	0	-	-	-	*				
	8	0	0	100	100	0	*			
	13	0	0	0	0	0	0	*		
	14	0	-	93	-	-	100	0	*	
	15	0	-	0	-	100	0	0	0	*

* Donor and recipient insertion sites are identical.

\- Not determined

Tn*5*-B20 Mutagenesis of Plasmids

Tn*5*-B20 insertions on pZT26 and pZT31 were identified by triparental mating of the plasmids from the donor *E. coli* strains into strains Rm11382 and Rm11374 recipients respectively using *E. coli* MT616 as mobilizer. The $Sm^rNm^rTc^r$ transconjugants obtained were screened for ability to grow on minimal medium with acetate as a sole carbon source, and five insertions that disrupted the complementing ability of pZT26 and pZT31 were retained. These Tn*5*-B20 insertions were then tested for *lacZ* expression in the Lac strain Rm8501 and Lac^+ strains were chosen. The precise locations of these insertions were determined by sequence analysis using the IS*50* primer.

DNA Sequence Analysis

Comparison of the restriction analysis of the original and transposon-mutagenized complementing clone (data not shown) identified the particular fragment actually responsible for phenotypic complementation. The region flanking *ace*::Tn*5*-B20 was subcloned from the transposon-mutagenized plasmid as a Km^r *Eco*RI fragment into pUC18. Each of the subclones was partially sequenced using the IS*50*-specific primer, yielding sequence directly in the flanking chromosomal DNA (Table 3.5). The *pod* sequence (determined previously in our laboratory) was from a Tn*5*, and not a Tn*5*-B20 insertion. Nucleotide and deduced amino acid sequences are shown in Figures 3.1 and 3.2.

Translated sequences from *ace5*::Tn*5*-B20 (group IV) exhibited strong homology to anaerobic coproporphyrinogen III oxidase (*hemN*). Comparison of the query sequence (150 amino acids) with GenBank revealed sequences homologous to the coproporphyrinogen III oxidase enzyme from *B. japonicum* (GenBank accession number AJ002517), which contributed to a sequence identity of 45% (64% similarity).

Translated sequences from *ace15*::Tn*5*-B20 (group III) exhibited strong homology to acetyl-CoA synthetase. The query sequence (217 amino acids) showed a

sequence identity of ca. 65% (79% similarity) to the acetyl-CoA synthetase enzyme from *E. coli* (GenBank accession number AAC77039). An *acs* designation has already been used to describe the gene encoding acetoacetyl-CoA synthetase in *S. meliloti* (16). For this reason the acetoacetyl-CoA synthetase was termed *acsA* and the acetyl-CoA synthetase was termed *acsB*. Alignment of the deduced amino acid sequences of AcsB with the *S. meliloti* AcsA protein (GenBank accession number AF080217) revealed they were significantly similar.

GenBank searches with sequences from *ace13*::Tn*5* (group II) in pZT14 revealed a reading frame with strong homology to the pyruvate orthophosphate dikinase (PPDK) protein, encoded by the *pod* gene, from other organisms (108). Comparison of the query sequence (261 amino acids) with that of high score database sequences revealed long stretches of homologous sequences to the pyruvate orthophosphate dikinase enzyme from *Bacteroides symbiosum* (GenBank accession number AAA22917), which contributed to an overall sequence identity of about 59% (80% similarity).

Unfortunately no sequences were obtained from *ace1* due to difficulty in obtaining satisfactory transposon mutagenized clones for sequencing, and sequencing of *ace4* was not attempted.

Genetic Mapping

One representative from each mutant group was used to map the acetate mutations on the chromosome. Tn*5-mob* donor strains were crossed with one mutant from each group. Transconjugants arising after selection for Rf^r Gm^r Sp^r were scored, and divided by the number of Rf^r recipient cells to determine conjugation frequency (Table 3.6). The chromosomal location of the mutation was estimated to be close to the insertions from which it is transferred at the highest frequency. Figure 3.3 shows the positions of the acetate mutations on the chromosome. The *acsB*::Tn*5*-233 insertion mapped to the chromosome. The *acsA* gene was previously shown to map to the chromosome as well (17).

Table 3.5. Molecular characterization of *ace* mutations

Query sequence[a]	Length of sequence (amino acids)	Gene	Sequences producing high scoring segment pairs*	
			Protein product	Probability
ace5::Tn*5-B20*	150	*hemN*	Anaerobic coporphyrinogen III oxidase (*Bradyrhizobium japonicum*)	1.2e-28
			Anaerobic coporphyrinogen III oxidase (*Rhodobacter sphaeroides*)	8.1e-12
			O_2-independent coporphyrinogen III dehydrogenase (*Ralstonia eutropha*)	2.6e-07
			O_2-independent coporphyrinogen III dehydrogenase (*Salmonella typhimurium*)	4.7e-05
ace15::Tn*5-B20*	217	*acs*	Acetyl-Coenzyme A synthetase (*Escherichia coli*)	1.2e-55
			Acetyl-Coenzyme A synthetase (*Phycomyces blakesleeanus*)	1.9e-43
			Acetyl-Coenzyme A synthetase (*Arabidopsis thaliana*)	8.4e-43
			Acetyl-Coenzyme A synthetase (*Penicillium chrysogenum*)	1.5e-40
			Acetyl-Coenzyme A synthetase 2 (*Saccharomyces cerevisiae*)	4.0e-40
ace13::Tn*5*	261	*pod*	Pyruvate orthophosphate dikinase (*Bacteroides symbiosum*)	4.5e-29
			Pyruvate orthophosphate dikinase (*Entamoeba histolytica*)	1.6e-26
			Pyruvate orthophosphate dikinase (*Zea mays*)	2.3e-19
			Pyruvate orthophosphate dikinase (*Flaveria trinerbia*)	2.0e-18
			Pyruvate orthophosphate dikinase (*Giardia intestinalis*)	3.7e-18

[a]Region flanking the *ace* mutation

*Obtained from similarity searches in GenBank

Table 3.6. Conjugal mapping of acetate mutations in *S. meliloti*

Allele	Relevant characteristics	Number of transconjugants per 10^8 recipient cells						
		H347	H348	H349	H350	H351	H352	H353
ace1	(*ace1*, group I)	0	0	0	0	3767	0	0
ace5	(*hemN*, group IV)	1082	0	0	0	0	0	0
ace13	(*pod*, group II)	0	0	954	0	0	1142	0
ace15	(*acsB*, group III)	0	0	0	1081	0	0	0

Conjugal matings were performed as described in Materials and Methods. The recipient strain was Rm5000. Recombinants were selected for Rf^r Gm^r Sp^r.

Strain number identifies mapping strains; for example, H347 is RmH347.

See Figure 3.3 for position of acetate mutations on the chromosome.

Growth Experiments

Growth tests were carried out for representative mutants in liquid culture to confirm the growth phenotypes observed on agar-solidified media. Mutants were grown in different carbon sources (see Figure 3.4). Growth of all mutants on glucose, succinate, glycerol and lactate was similar to that of the wild-type control. All the *ace* mutants showed little or no growth on acetate, acetoacetate and 3-hydroxybutyrate with the exception of *ace15*::Tn*5* (*acsB*) which grew to the same extent as the wild type on acetoacetate and 3-hydroxybutyrate. The growth rate of the *acsB* mutant strain on acetate was reduced compared to wild type but eventually reached the same cell density (mean generation times of 39 and 10 hours respectively).

To further characterize the phenotype of *ace* mutants, they were grown in minimal media supplemented with a range of acetate concentrations (see Figure 3.5). *E. coli acs* mutants grow poorly on low concentrations of acetate (≤10 mM) whereas *ack* and *pta* mutants are not affected for growth on acetate at these concentrations (65). All the acetate mutants characterized in this study grew as well as the wild type on glucose medium alone and on glucose with acetate. This suggested that none of the mutants were inhibited for growth by the presence of acetate. All the mutants, with the exception of *ace15*::Tn*5* (*acsB*), showed little or no growth at the various acetate concentrations.

ace15::Tn*5* (*acsB*) was able to grow at very low concentrations of acetate (2.5 mM-10 mM) but not at higher acetate concentrations (30 mM-50 mM). When *ace15*::Tn*5* (*acsB*) was grown on 2.5 mM acetate, it had a shorter lag period than when it was grown on 10 mM acetate, as well as a shorter generation time (ca. 28 and 45 hours respectively).

E. coli mutants that were unable to grow on either acetate or oleate as a sole carbon source due to a defect in isoleucine-valine biosynthesis have been described (26). Such mutants were acetate auxotrophs rather than acetate utilization mutants. We tested whether an amino acid combination of isoleucine and valine stimulated the growth of the *ace* mutants on acetate, and found that when isoleucine and valine were supplemented into acetate minimal medium (see Table 3.7 and Figure 3.6), there was no improvement in the growth of any of the mutants. Interestingly, all of the mutants except for *ace15*::Tn*5* (*acsB*) showed a slight improvement in growth when acetate was supplemented with succinate. If mutants are defective in the expression of one or more enzymes of the glyoxylate shunt, they should be able to grow on acetate supplemented with any of the several end products of the glyoxylate shunt, such as succinate (26). This suggests that the phenotype of these mutants might, in some way, be related to the glyoxylate shunt.

Table 3.7. Growth rates of mutant and wild-type strains

		Generation time (h) at 30°C				
Strain		Glu	Ace	Ace + ILV	Ace + Succ	Ace + Succ + ILV
Rm1021	wild type	12.8	13.2	12.7	16.9	17
Rm11106	*ace1*	11.8	80.5	65.4	20.3	20.3
Rm11374	*hemN*	13.5	94.3	152.4	27.6	32.5
Rm11200	*pod*	12.8	112.7	152.3	25.8	22.9
Rm11382	*acsB*	14.1	32.7	25.4	33.8	33.8

Glu, glucose; Ace, acetate; Suc, succinate; ILV, isoleucine and valine.

Glucose and acetate were used at a concentration of 15 mM.

Succinate was added as a supplement at a concentration of 0.02%.

Isoleucine and valine were added at concentrations of 20 and 17 μg/ml respectively.

Growth Competition Tests

The ability of *S. meliloti* to survive the varying nutrient supply in the rhizosphere, and compete against other strains for nodule occupancy, are important determinants for the establishment of a successful symbiosis. Other carbon metabolism mutants have been shown to be affected in growth competition and/or symbiotic competition (3, 81, 117). To check the competitiveness of *ace* mutants with the wild type under conditions of fluctuating carbon availability, they were grown with the wild type (in a 1:1 ratio) in low and high carbon (glucose) and changes in proportion were followed over a period of four cycles (Figure 3.7a). The *ace1* mutant did show a 20% reduction over the four cycles. *ace13* showed a 20% reduction and *ace15* a 17% reduction over the four cycles. If we examine growth of the strains alone in monoculture, the wild type and mutants all seem to decrease in number over the course of the experiment (Figures 3.7b and 3.7c).

Assay for Isocitrate Lyase and Malate Synthase Activity

Since no glyoxylate shunt mutations have been characterized in *S. meliloti*, the *ace* mutants were assayed for isocitrate lyase and malate synthase activities. Similar mutants in *S. typhimurium* were found to have defects in the glyoxylate shunt (118). The formation of isocitrate lyase in many organisms is known to be greatly influenced by the nature of the carbon source utilized for growth. In *S. meliloti* isocitrate lyase is induced during growth on acetate (75). The cells for the enzyme assay were grown in TY medium supplemented with 10 mM glucose. All the strains did show isocitrate lyase activity (Figure 3.8). The *ace1* and *pod* mutants had activity similar to the wild type while the other strains had activity significantly higher than the wild type. In the *hemN* mutant, the activity was much higher, perhaps reflecting compensation for its mutation. Although *ace8* and *ace14* mutations were placed in group IV with *hemN*::Tn*5*, they did not show similar increases in isocitrate lyase activity.

The Acetate Utilization Phenotype of the *pod* Mutant

The isolation of a *S. meliloti pod* mutant in the study by Østerås and colleagues (82) is illustrated in Figure 3.9. This *pod* mutant was reported to be Ace^+ (82); during studies with *pckA*, a mutant was isolated which grew normally on succinate minimal medium because of a second-site suppressor mutation *spk*. Tn*5* insertions that abolished the suppressor phenotype were found within the *pod* gene, suggesting at that time that the suppressor mutation was within *pod*. The phenotype of this *pod* mutant contrasted with the Ace^- phenotype of the *pod* mutant isolated previously in our laboratory. The sequences from the two mutants, aligned with the *pod* gene of *B. symbiosum*, indicate the position of Tn*5* in the gene (Figure 3.10).

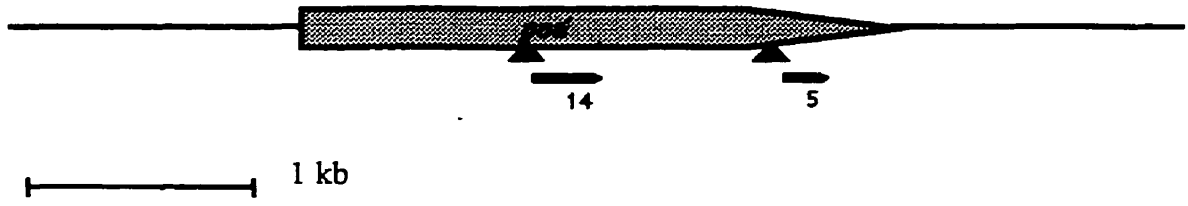

Figure 3.10. Sequence alignment of *Bacteroides symbiosum pod* gene (86) with query sequences from *S. meliloti*. The bars show the alignment of DNA sequences from *S. meliloti pod* with the *pod* gene from *B. symbiosum*. The arrows show the location of Tn5 insertions within the *pod* gene. *pod5* sequence was from a previous study (82). *pod14* sequence was isolated in our laboratory.

Before resolving the differing phenotypes of the two *pod* mutants, it had to be confirmed that the Tn*5* insertion in pZT14 was near the site of the original gene insertion. Tn*5* mutagenesis of pZT9 (complementing clone of *ace13*::Tn*5* (*pod*)) gave rise to pZT14 that was unable to complement *ace13*::Tn*5* (*pod*). Sequences, with homology to *pod*, were obtained from the region flanking the insertion in pZT14. These sequences are

indicated as *pod14* in Figure 3.10. The insertion from the pZT14 was recombined into the *S. meliloti* chromosome. The resulting homogenote Rm11314 exhibited an Ace$^-$ phenotype. The insertion in Rm11314 was transduced into Rm11244 (*ace13*::Tn*5*-233) and the two insertions were 100% linked. This indicated that Tn*5* in pZT14 was located very close to the site of the original insertion.

It could be hypothesized that the *pod* mutant isolated by Østerås *et al.* still contained the suppressor mutation. It might be possible that the *spk* mutation was in fact closely linked to *pod* but not actually in *pod*, and that *pckA* suppression requires *pod*. Therefore if *pod* is knocked out, *pckA* would not be suppressed. In addition, the *spk* mutation somehow requires *pod* for phenotypic expression.

The *pod* mutant RmG274 (*pod5*::Tn*5*), which was believed to carry the suppressor, was obtained. The *pod5*::Tn*5* mutation was transduced into wild-type Rm1021, selecting for Nm^r. 4 out of 170 transductants screened were Ace$^-$. This meant that the suppressor was so tightly linked that 98% of the time, it was contransduced with the Tn*5*. Growth of two Ace$^-$ transductants (Rm11327, Rm11328) and two Ace$^+$ transductants (Rm11338, Rm11339) from this experiment are shown in Figure 3.11.

Strain RmG139 carrying only the suppressor mutation *spk* was also obtained. Tn*5* in *ace13* was transduced into RmG139. All 375 transductants screened were Ace$^-$ (100% linked).

Studies had also suggested that *pod* plays a role in the suppression of the *pckA* phenotype. When the wild-type *pod* cosmid clone (pZT9) was transferred into the *pckA* mutant Rm5439, it was able to grow on succinate minimal medium. To confirm the growth phenotypes, growth tests were performed in liquid culture. Figure 3.12 shows growth of the RmG274 (the *pod* mutant isolated previously), Rm11200 (*pod* mutant in this study), RmG139 (strain carrying the suppressor mutation *spk*), Rm5439 (*pckA* mutant), and Rm5439 carrying the *pod* cosmid clone pZT9. If a strain is able to grow on pyruvate, it is generally able to grow on lactate as well. The *pckA* strain shows very poor growth on pyruvate and lactate (82). The *pckA* mutant carrying the clone complementing the Ace$^-$ phenotype of Rm11200 grew with a slightly longer generation time on succinate than the wild type (5.4 hours compared to 4.3 hours for the wild type).

Tn*5*-B20 mutagenesis of pZT9 generated clones that failed to complement the Ace⁻ phenotype of Rm11200 and formed blue colonies on LB X-gal medium. The insertion in the resulting plasmid, pZT40, was then recombined into the *S. meliloti* genome (Rm8501, Lac⁻ background). The recombinant strain, Rm11358, was unable to utilize acetate. To see if the expression of *pod* depended upon the carbon source and/or growth phase, β-galactosidase activity was measured over the complete growth cycle of Rm11358 with pZT9 growing in M9 glucose, M9 succinate and M9 acetate. Rm8501 carrying pZT9 was the strain used as a control for background activity. pZT9 had to be present because otherwise Rm11358 would not grow on acetate minimal media. To ensure plasmid maintenance in test strains, Tc was used at a low concentration of 2 μg/ml. In all carbon sources, induction was observed very early and increased steadily during the log phase (Figure 3.13); no further increase in expression was observed in the stationary phase. The expression of *pod* was similar in all three carbon sources.

Phenotypic Analysis of the *acsB* Mutant

The mutation in Rm11382 (*ace15*::Tn*5*) was found to be within the gene encoding acetyl-CoA synthetase (*acs*). Another *S. meliloti acs* gene encoding acetoacetyl-CoA synthetase had been isolated in our laboratory and designated *acsA* (14). The new gene was thus designated *acsB*. The complete nucleotide sequence is available for the *acsA* gene (16). Sequence alignment of a portion of the Acs proteins from *S. meliloti* and *E. coli* is shown in Figure 3.14. Transduction tests showed that the two *S. meliloti acs* genes were not linked (data not shown). The phenotypes of the two mutants were distinct. A double mutant with mutations in both *acs* genes was constructed (Rm11364) and growth tests were performed (Figure 3.15). The growth of the *acsA* mutant, *acsB* mutant and the double mutant on glucose was comparable to that of the wild type. The *acsA* mutant (Rm11134) did not grow on acetoacetate and 3-hydroxybutyrate. However, it grew as well as the wild type on acetate. The *acsB* mutant, as seen in the previous growth experiments, grew on acetoacetate and 3-hydroxybutyrate as well as the wild type and on acetate with a longer generation time. The double mutant shared the phenotypes of both

individual strains. It did grow very slowly on acetate and not at all on acetoacetate and 3-hydroxybutyrate.

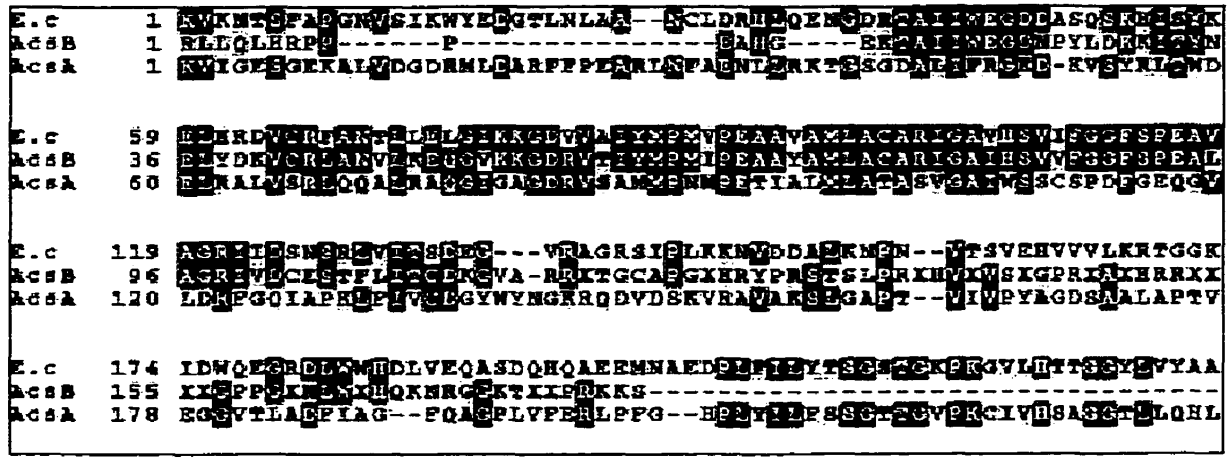

Figure 3.14. Alignment of part of the AcsB protein (210 aa) with the AcsA protein (650 aa) of *S. meliloti* and Acs protein (651 aa) of *E. coli* (E. c in the figure). Alignment was performed using the ClustalW program. Amino acids that are identical between the aligned sequences are shaded dark grey. Light grey shading represents amino acids with similar functional groups. The non-shaded areas indicate dissimilar amino acids. The partial sequence of AcsB was 65% identical to the *E. coli* Acs polypeptide and 34% identical to the *S. meliloti* AcsA polypeptide.

Biochemical Characterization of the *acs* Mutants

The levels of ACS and AACS were determined in cell extracts of *acsA*, *acsB* and *acsA acsB* mutants (Figures 3.16 and 3.17). The three mutant strains had lower ACS and AACS activities than the wild type. The single mutations seem to affect both ACS and AACS activities. However, the *acsA* mutant had 60% more ACS activity than the *acsB* mutant and the *acsB* mutant had 50% more AACS activity than the *acsA* mutant.

Figure 3.1. Nucleotide and deduced amino acid sequence of the 465 bp fragment flanking the Tn*5*-B20 from pZT38. GenBank searches with these sequences revealed reading frames with strong homology to the anaerobic coproporphyrinogen III oxidase from other organisms.

```
        10         20         30         40         50
ACGTTACCTCGTTAGGAGGTCACATGGAANATCAGATCCTGGAAAACGGG
 T  L  P  R  *  E  V  T  W  X  I  R  S  W  K  T  G>

        60         70         80         90        100
AAAGGTTCCGTTCAGGACGCTACTTGTGTATAAAANTCAGGTGCAGAACG
  K  V  P  F  R  T  L  L  V  Y  K  X  Q  V  Q  N>

       110        120        130        140        150
AGGTGCCGCCGGGCCTCTACGCCCAACACATAGCCTCGGGTCGGCTTGCA
E  V  P  P  G  L  Y  A  Q  H  I  A  S  G  R  L  A>

       160        170        180        190        200
ACGGTGAAAGGCTACCGGATGACGCCCGAGGATAGACTGCGGGCAGGCAT
 T  V  K  G  Y  R  M  T  P  E  D  R  L  R  A  G  I>

       210        220        230        240        250
CATCGAGCGGCTGATGTGCGACTTCGGCGTCGATGTTCCCGCCCTTGCCA
  I  E  R  L  M  C  D  F  G  V  D  V  P  A  L  A>

       260        270        280        290        300
CCGCGCACGGGTTCGATCCGGAGATGCTGCTCCGCGGCAACACCAGGCTC
T  A  H  G  F  D  P  E  M  L  L  R  G  N  T  R  L>

       310        320        330        340        350
GCTATGCTGGAAAGTGATGGCATCCTTGATATCGCTGACGGCGTCATACG
 A  M  L  E  S  D  G  I  L  D  I  A  D  G  V  I  R>

       360        370        380        390        400
GCTGCGCGAGGGGCGACNCTTCCTTNTCCGCGCCGCCGCTGCAGCCTTCG
  L  R  E  G  R  X  F  L  X  R  A  A  A  A  A  F>

       410        420        430        440        450
ACGCCTATATCGAACAATCGGGACGGACGCATAGCAAGGCGGCGTTGAAA
D  A  Y  I  E  Q  S  G  R  T  H  S  K  A  A  L  K>

       460
GCCGCATCAAGCTGA
 A  A  S  S  *>
```

Figure 3.2. Nucleotide and deduced amino acid sequence of the 631 bp fragment flanking the Tn*5*-B20 from pZT39. GenBank searches with these sequences revealed reading frames with strong homology to the acetyl-CoA synthetase enzyme from other organisms.

```
        10         20         30         40         50
AGTCAGGTTCGAGCCCTATACCAAGGTCAAGAACACGTCCTTCGAGGGCG
 S  Q  V  R  A  L  Y  Q  G  Q  E  H  V  L  R  G  R>

        60         70         80         90        100
ATGTCTCGATCAAGTGGTTCGAANACGGACTGACCAACGTCTCCTACAAT
   C  L  D  Q  V  V  R  X  R  T  D  Q  R  L  L  Q>

       110        120        130        140        150
TGCATCGACCGCCACCTGAAGACGCACGGCGAAAAGACGGCGATCATCTG
L  H  R  P  P  P  E  D  A  R  R  K  D  G  D  H  L>

       160        170        180        190        200
GGAGGGAGACAATCCCTATCTCGACAAGAAGATCACCTATAACGAGCTCT
G  G  R  Q  S  L  S  R  Q  E  D  H  L  *  R  A  L>

       210        220        230        240        250
ACGACAAGGTTTGCCGTCTTGCCAACGTCTTGAAGGAGCAGGGCGTAAAG
   R  Q  G  L  P  S  C  Q  R  L  E  G  A  G  R  K>

       260        270        280        290        300
AAGGGGGACCGCGTCACCATCTACATGCCGATGATCCCGGAAGCAGCCTA
E  G  G  P  R  H  H  L  H  A  D  D  P  G  S  S  L>

       310        320        330        340        350
TGCGATGCTCGCCTGTGCCCGCATCGGCGCGATCCATTCGGTCGTTTTCG
C  D  A  R  L  C  P  H  R  R  D  P  F  G  R  F  R>

       360        370        380        390        400
GCGGCTTTTCGCCCGAGGCGCTCGCCGGCCGCATCGTCGATTGCGAGTCC
   R  L  F  A  R  G  A  R  R  P  H  R  R  L  R  V>

       410        420        430        440        450
ACCTTCCTGATCACCTGCGACAAAGGCGTTGCGCGGCGGCNAACCGGTTG
H  L  P  D  H  L  R  Q  R  R  C  A  A  A  N  R  L>

       460        470        480        490        500
CGCTCCAGGANAACACCGATACCCGCGATCGACATCGCTGCCCAGANAGC
R  S  R  X  T  P  I  P  A  I  D  I  A  A  Q  X  A>

       510        520        530        540        550
ACGTCNCGGTCAGCAANGGTCCTCGTCNTGCGCCNCACCGGCGGNAANGT
   R  X  G  Q  Q  X  S  S  S  C  A  X  P  A  X  X>

       560        570        580        590        600
CNGNTGGGGCCCCCGGGCCNCAATCTCTGGTNTCACCAGAAAAACCGCGG
S  X  G  A  P  G  P  Q  S  L  V  S  P  E  K  P  R>

                  610        620        630
            CGGCAAAACCNCNTGNCCCCGGAAAAAATCC
             R  Q  N  X  X  X  P  E  K  I  X>
```

Figure 3.3. Chromosomal map of *S. meliloti* showing locations of Tn*5-mob* insertions and the relative positions of the *ace* mutations. The seven Tn*5-mob* strains are Hfr-like strains, which are Nm^r and carry the origin of transfer (*oriT*) of plasmid RP4 in different positions and/or orientations. The arrows show the origin and direction of transfer. The location of some other genes are also shown for reference. *ace13*::Tn*5* was within pyruvate orthophosphate dikinase and *ace15*::Tn*5* was within acetyl-CoA synthetase. The location of *ace5* was not determined. However *ace14* (location determined) was 93% linked to *ace5*. *ace1* was not sequenced.

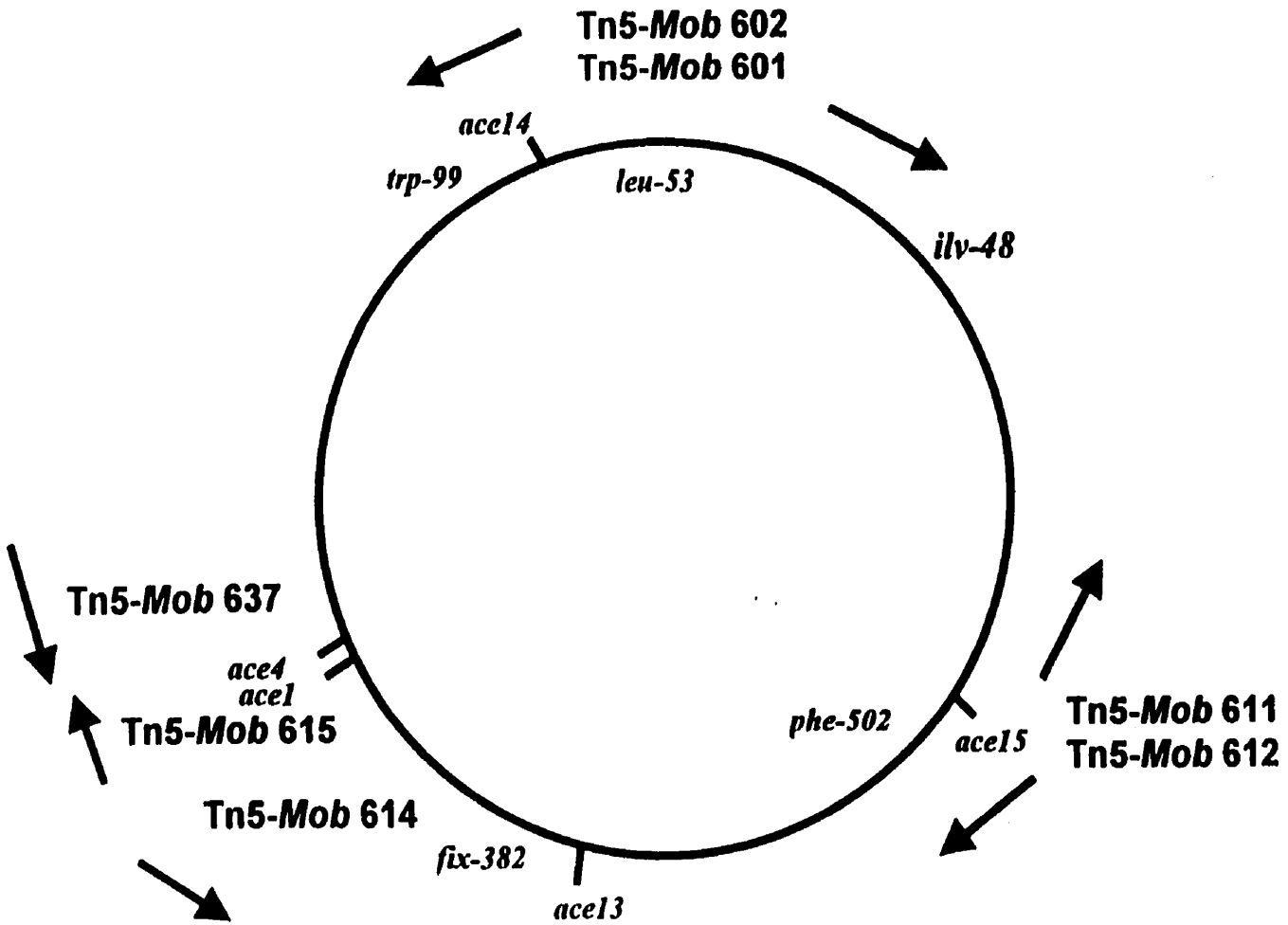
Tn5-Mob 602
Tn5-Mob 601
ace14
trp-99
leu-53
ilv-48
Tn5-Mob 637
ace4
ace1
Tn5-Mob 615
Tn5-Mob 614
phe-502
ace15
Tn5-Mob 611
Tn5-Mob 612
fix-382
ace13

Figure 3.4. Comparison of the growth kinetics of the wild-type strain and representative mutants on different carbon sources. Strains used were Rm1021 (wild type), Rm11106 (*ace1*::Tn*5*), Rm11374 (*hemN*::Tn*5*), Rm11200 (*ace13*::Tn*5*) and Rm11382 (*acsB*::Tn*5*). Carbon sources were used at the following concentrations (mM): Glucose, 10; Succinate, 15; Acetate, 30; Acetoacetate, 15; 3-Hydroxybutyrate, 15; Glycerol, 20; Lactate, 20. The growth of each culture was followed for 190 hours or until stationary phase was reached. ♦, wild type; ×, *ace1*; ■, *hemN*; ●, *ace13*; ▲, *acsB*.

Glucose

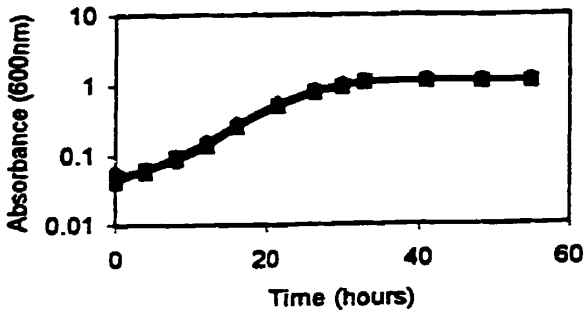

Succinate

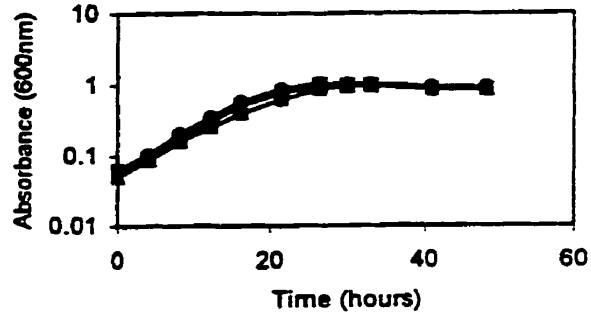

Acetate

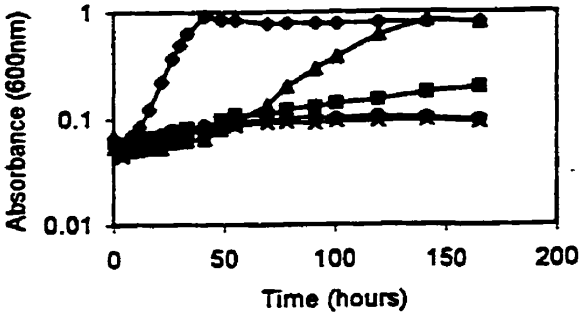

Acetocetate

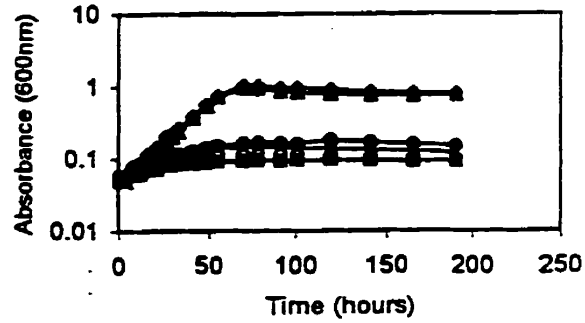

3-Hydroxybutyrate

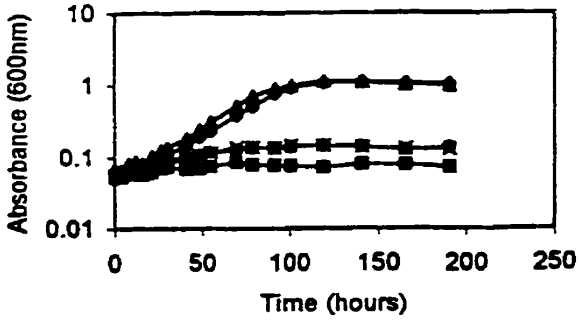

Glycerol

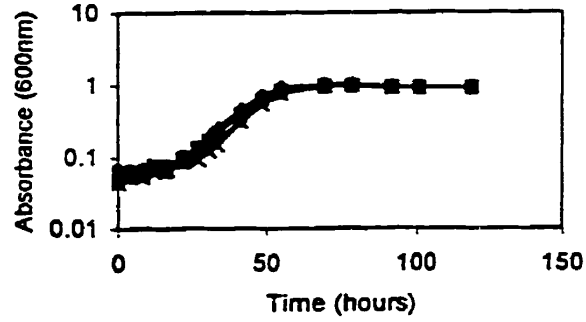

Lactate

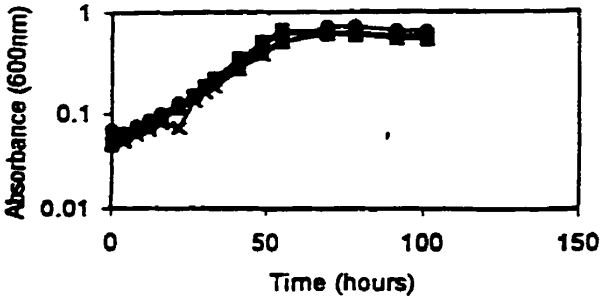

Figure 3.5. Comparison of the growth kinetics of the wild-type strain and representative mutants on different concentrations of acetate. Strains used were Rm1021 (wild type), Rm11106 (*ace1*::Tn*5*), Rm11374 (*hemN*::Tn*5*), Rm11200 (*ace13*::Tn*5*) and Rm11382 (*acsB*::Tn*5*). M9 minimal medium was supplemented with the indicated concentration of glucose and/or acetate. The growth of each culture was followed for 160 hours or until stationary phase was reached. ♦, wild type; ■, *ace1*; ∗, *hemN*; ×, *ace13*; ●, *acsB*.

Glucose 10mM

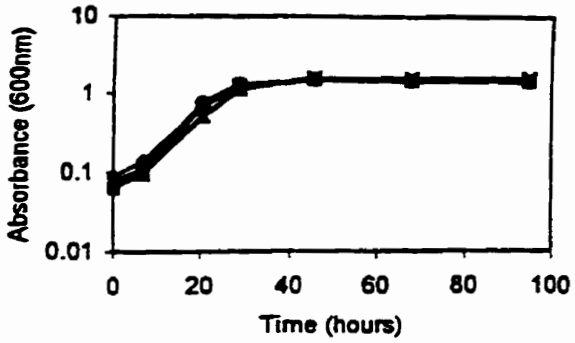

Glucose 10mM+Acetate 30mM

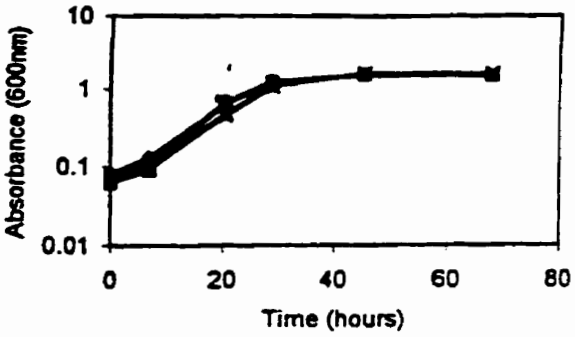

Acetate 2.5mM

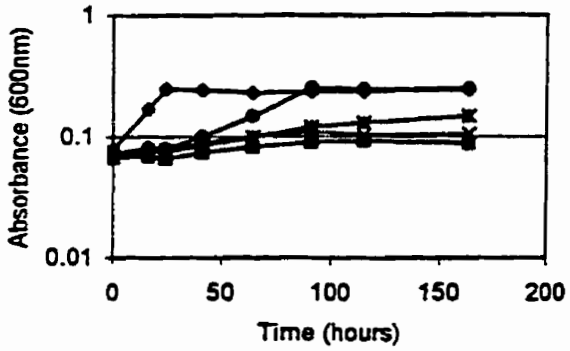

Acetate 10mM

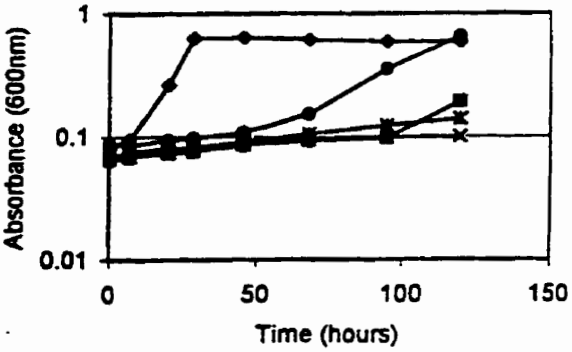

Acetate 30mM

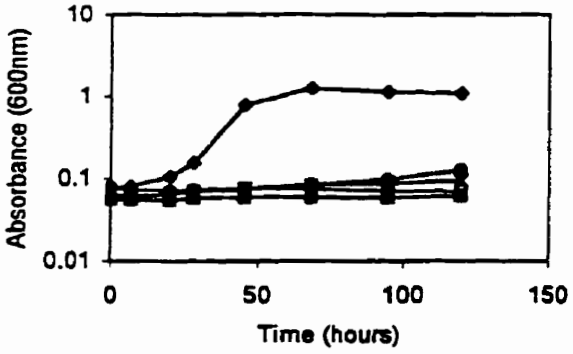

Acetate 50mM

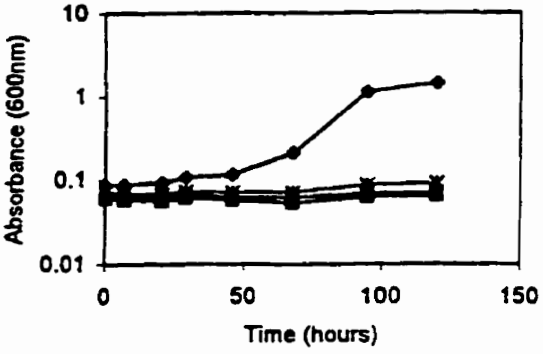

Figure 3.6. Comparison of the growth kinetics of the wild-type strain and representative mutants on acetate medium supplemented with amino acids and/or succinate. Strains used were Rm1021 (wild type), Rm11106 (*ace1*::Tn*5*), Rm11374 (*hemN*::Tn*5*), Rm11200 (*ace13*::Tn*5*) and Rm11382 (*acsB*::Tn*5*). Glucose and Acetate was used at a concentration of 15 mM. Isoleucine and valine were added at concentrations of 20 and 17 µg/ml respectively. Succinate was added as a supplement at a concentration of 0.02%. ◆, wild type; ■, *ace1*; ∗, *hemN*; ×, *ace13*; ●, *acsB*.

Glucose 15mM

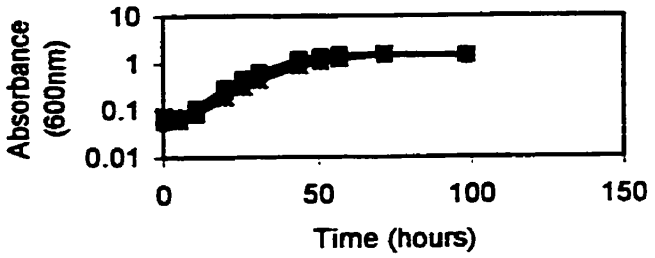

Acetate 15 mM

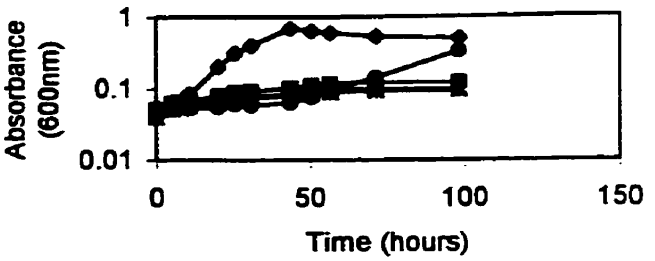

Acetate 15mM+ ILV

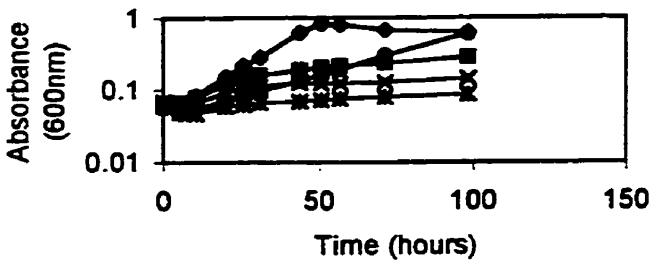

Acetate 15mM + Succinate 0.02%

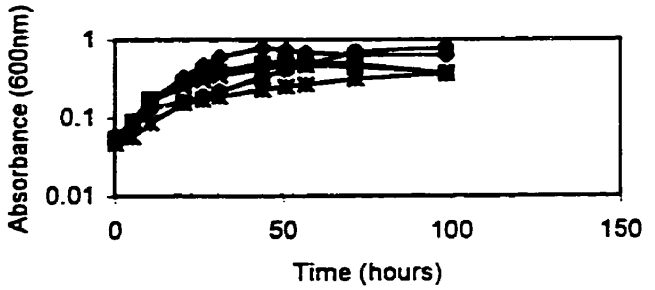

Acetate 15mM +Succinate 0.02%+ ILV

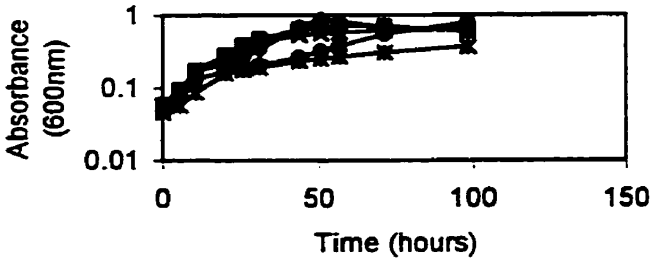

Succinate 0.02%

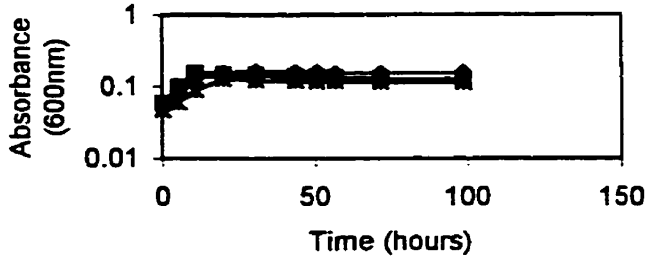

ILV

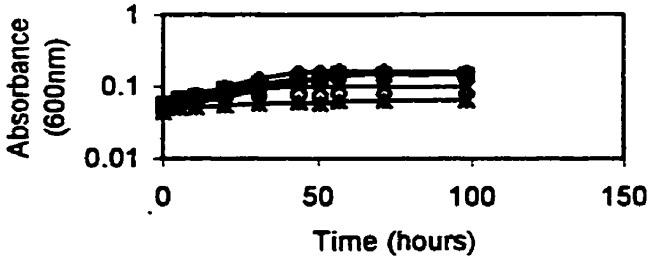

Succinate 0.02%+ ILV

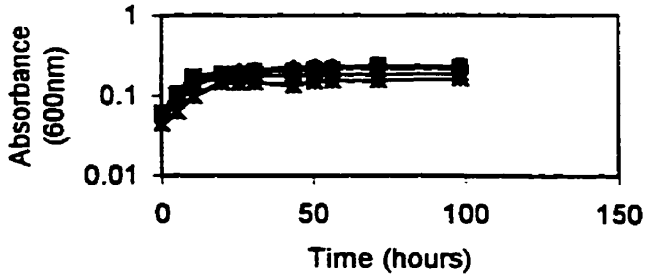

Figure 3.7. Growth competition assays of *S. meliloti* mutants co-inoculated (approx. 1:1) with the wild type. The cultures were subjected to growth in alternating carbon-rich (15 mM glucose) and carbon-poor (2.5 mM glucose) media. A 0.1 ml aliquot was withdrawn every 24 h and inoculated into 5 ml of M9-minimal medium supplemented with either 15 mM or 2.5 mM glucose as a sole carbon source. Another aliquot was withdrawn to determine total cfu/ml. Figure 3.7(b) shows the cfu/ml of the culture mix. Figure 3.7 (c) shows the cfu/ml of the individual strains over the course of the experiment. The fraction of the total population represented by the mutant strain (Figure 3.7(a)) was scored by screening 150 colonies for Nm^r. Culture mixes used were Rm1021: Rm11106 (Wild type: *ace1*::Tn*5*), Rm1021:Rm11200 (Wild type: *ace13*::Tn*5*) and Rm1021:Rm11382 (Wild-type: *acsB*::Tn5). Each data point represents an average of three independent mixed cultures.

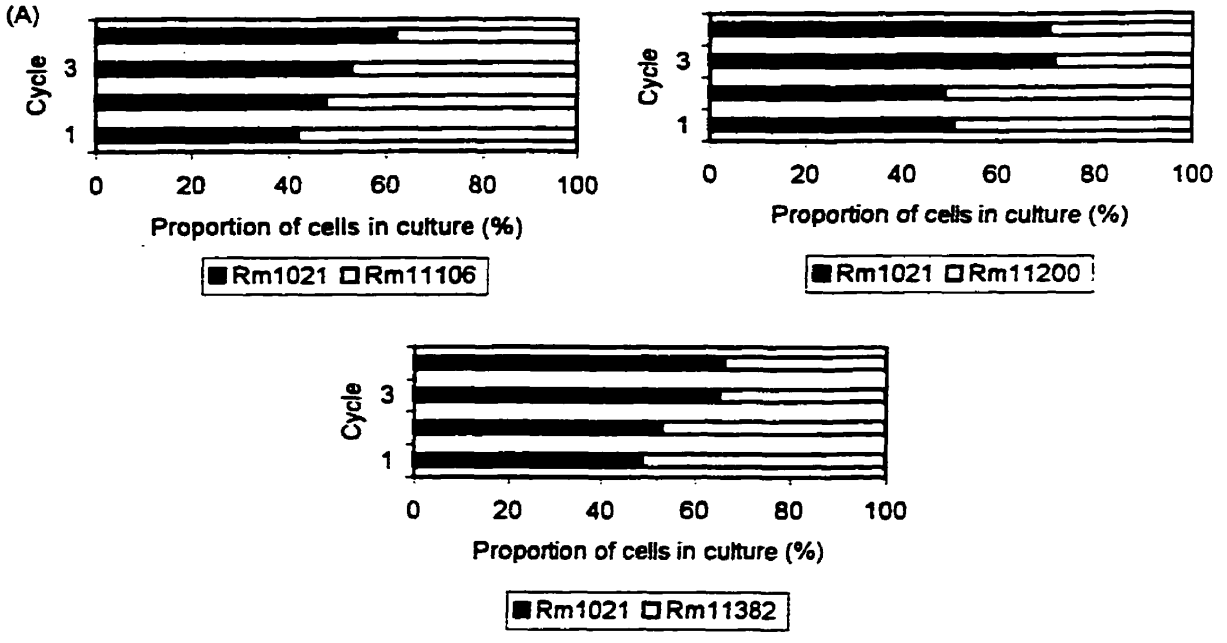
(A)
Cycle
3
1
0
20
40
60
80
100
Proportion of cells in culture (%)
Rm1021 Rm11106
Rm1021 Rm11200
Rm1021 Rm11382

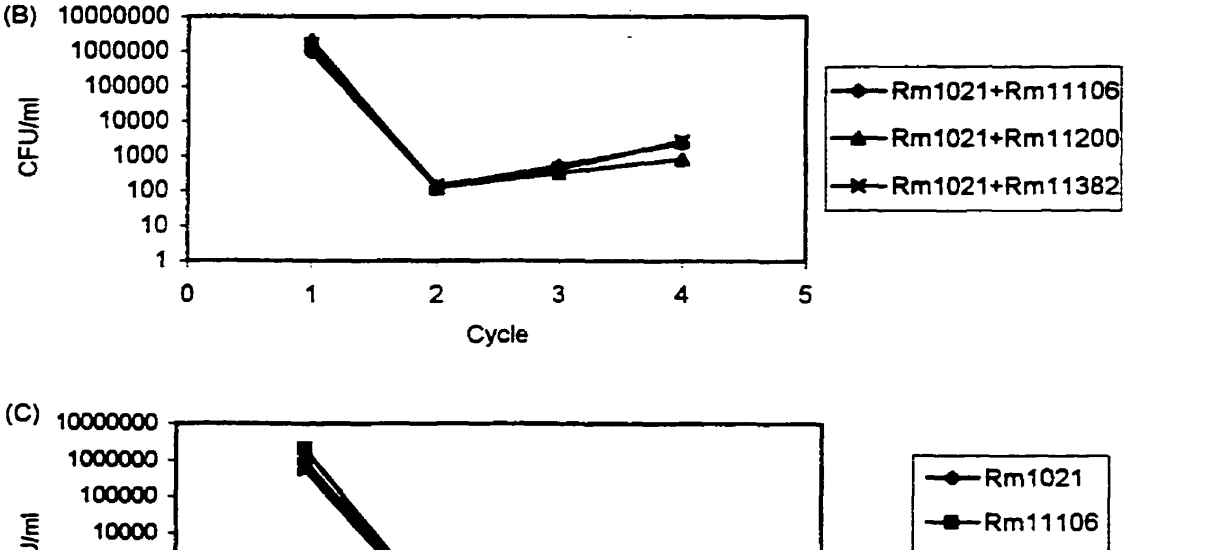
(B)
CFU/ml
10000000
1000000
100000
10000
1000
100
10
1
0
1
2
3
4
5
Cycle
Rm1021+Rm11106
Rm1021+Rm11200
Rm1021+Rm11382

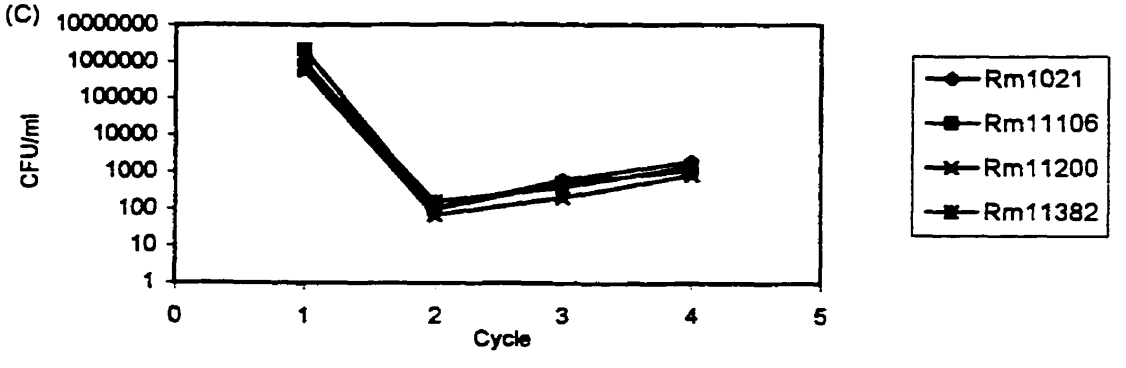
(C)
CFU/ml
10000000
1000000
100000
10000
1000
100
10
1
0
1
2
3
4
5
Cycle
Rm1021
Rm11106
Rm11200
Rm11382

Figure 3.8. Isocitrate lyase activities in cells of wild type and *ace* mutants grown on TY plus 10 mM glucose. Values represent average specific activity in crude extracts ± SE of triplicate assays. Strains used were Rm1021 (wild type), Rm11106 (*ace1*::Tn*5*), Rm11141 (*ace4*::Tn*5*), Rm11374 (*ace5*::Tn*5*), Rm11377 (*ace8*::Tn*5*), Rm11200 (*ace13*::Tn*5*), Rm11381 (*ace14*::Tn*5*) and Rm11382 (*ace15*::Tn*5*).

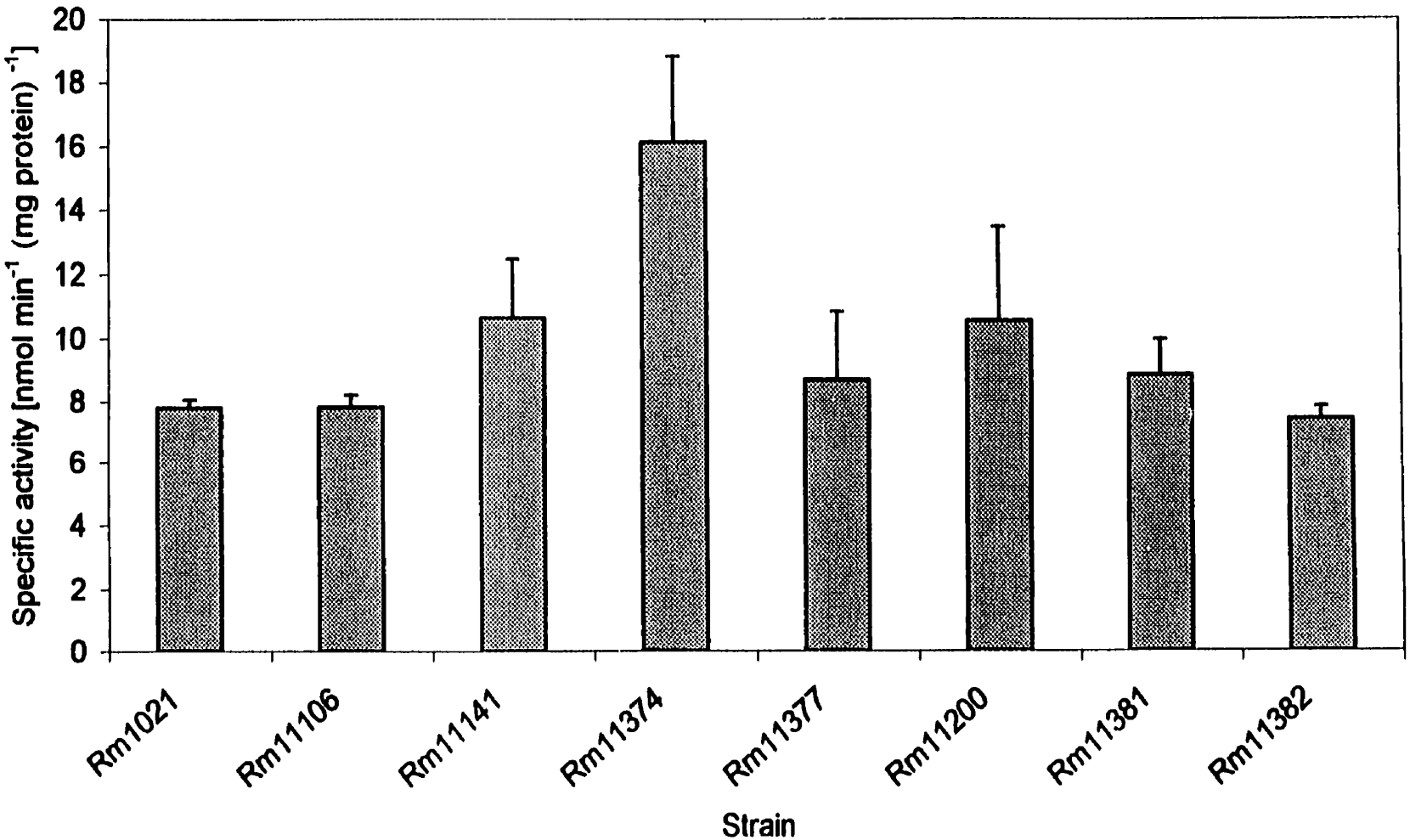
Specific activity [nmol min-1 (mg protein) -1]
20
18
16
14
12
10
8
6
4
2
0
Rm1021
Rm11106
Rm11141
Rm11374
Rm11377
Rm11200
Rm11381
Rm11382
Strain

Figure 3.9. Isolation of the *pod* mutant in previous study (82). The phenotype of the strain at each step is shown.

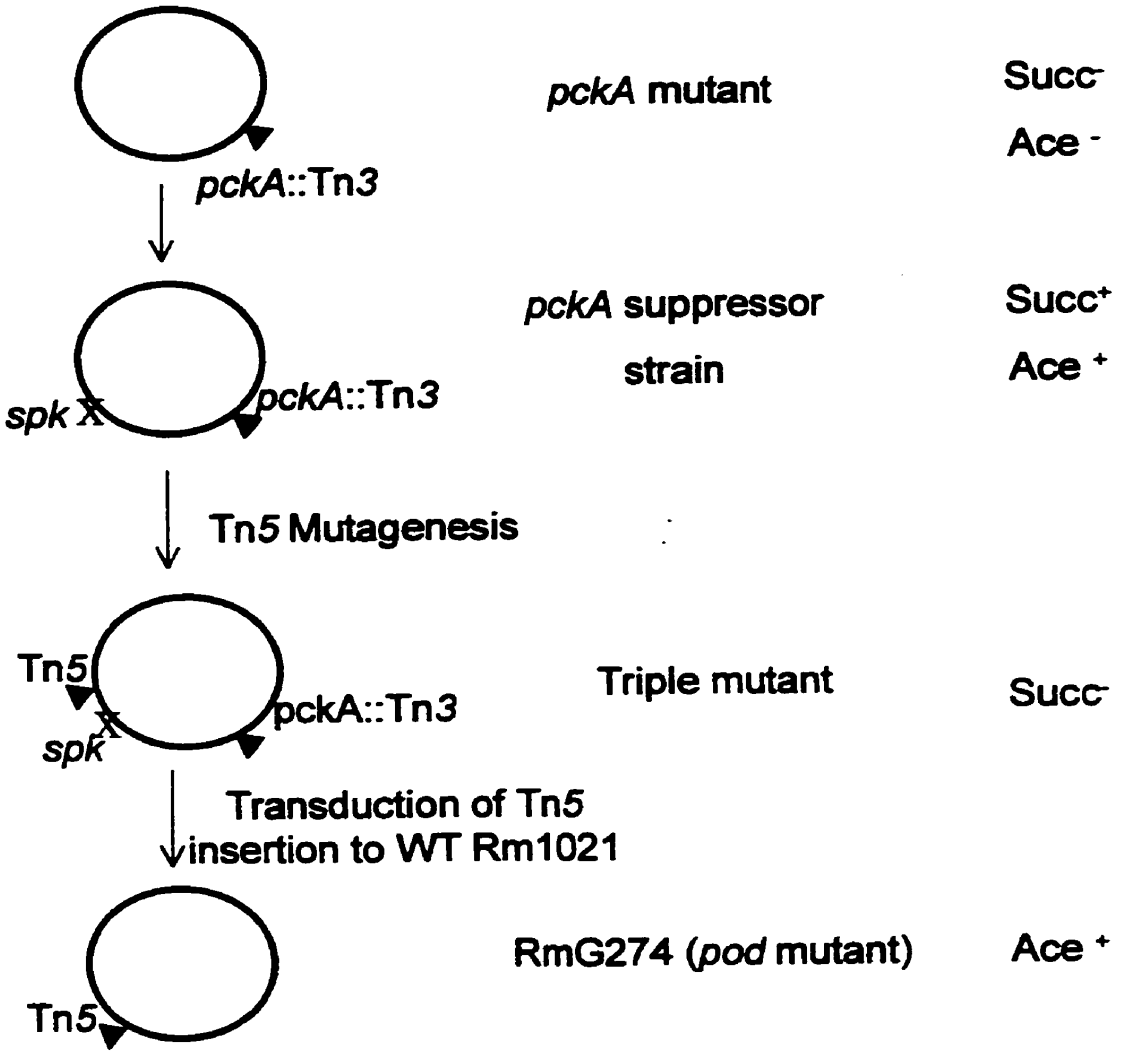
pckA mutant
Succ-
Ace -
pckA::Tn3
pckA suppressor
strain
Succ+
Ace +
spk
pckA::Tn3
Tn5 Mutagenesis
Tn5
spk
pckA::Tn3
Triple mutant
Succ-
Transduction of Tn5
insertion to WT Rm1021
RmG274 (pod mutant)
Ace +
Tn5

Figure 3.11. Growth of RmG274 (*pod5*::Tn*5*), Rm11200 (*ace13*::Tn*5*), Rm11327 (*pod*::Tn*5*), Rm11328 (*pod*::Tn*5*), Rm11336 (*pod*::Tn*5*), and Rm11337 (*pod*::Tn*5*) on acetate as the sole carbon source. The latter four strains were the result of the transduction of the Tn*5* insertion from RmG274 into wild-type Rm1021. 4 of the 170 transductants screened were Ace^-. Rm11327 and Rm11328 were Ace^-. Rm11338 and Rm11339 were Ace^+. The strains were streaked on TY plates as a control.

M9/Acetate
RmH338
RmH338
RmH338
RmH338
RmH338
RmH338

Figure 3.12. Comparison of the growth kinetics of the wild-type strain and representative mutants on different carbon sources. Strains used were Rm1021 (wild type), RmG274 (*pod5*::Tn*5*), RmG139 (*spk-1*), Rm11200 (*ace13*::Tn*5*), Rm5439 (*pckA1*::Tn*V*) with and without pZT9, and the complementing clone of Rm11200. All carbon sources were used at a concentration of 15 mM. The growth of each culture was followed for 72 hours or until stationary phase was reached. ♦, wild type; ■, *ace13*; Δ, *pckA1* (pZT9); ×, *pckA1*; ∗, *pod5*; ●, *spk-1*.

GLUCOSE

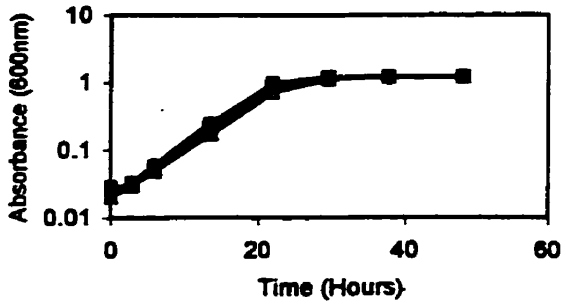

SUCCINATE

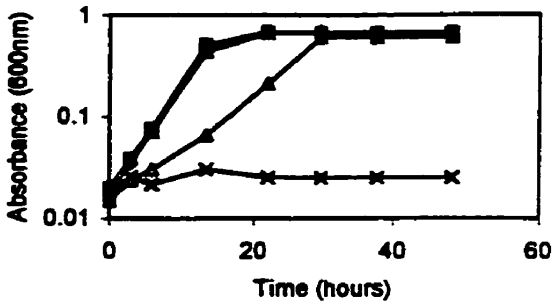

GLYCEROL

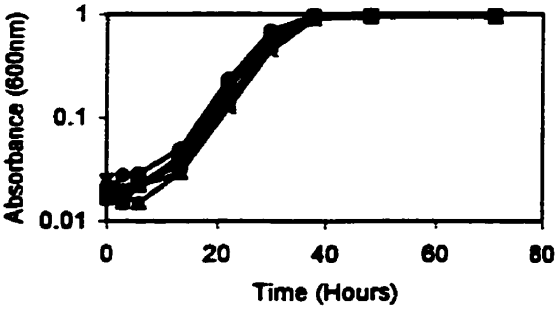

LACTATE

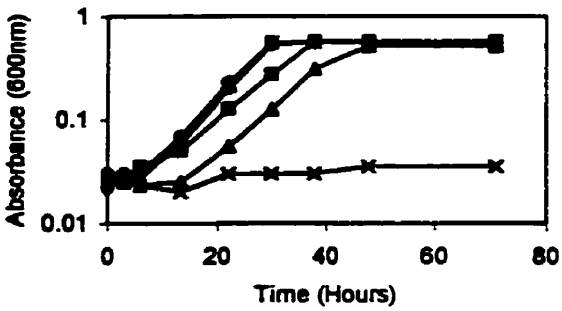

ACETATE

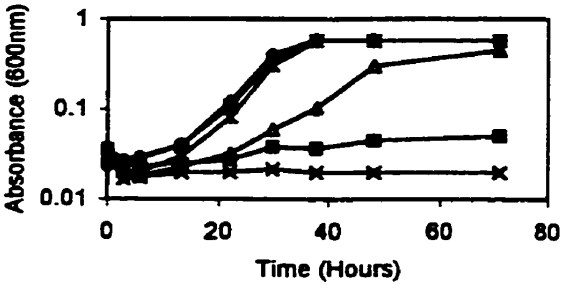

Figure 3.13. Relation between growth and *pod*::*lacZ* fusion expression in different media. Growth (shaded symbols) and β-galactosidase activity (open symbols) was measured for Rm11358 (*pod15*::Tn*5*-B20) carrying the pZT9 plasmid when grown on M9 acetate, M9 succinate and M9 glucose. Tetracycline was added at a concentration of 2 μg/ml to all M9 minimal carbon sources to maintain the plasmid in the test strain.

Acetate

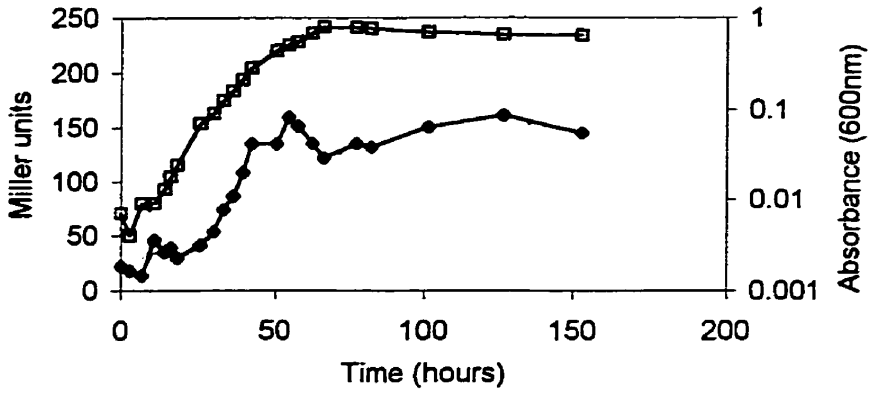

Succinate

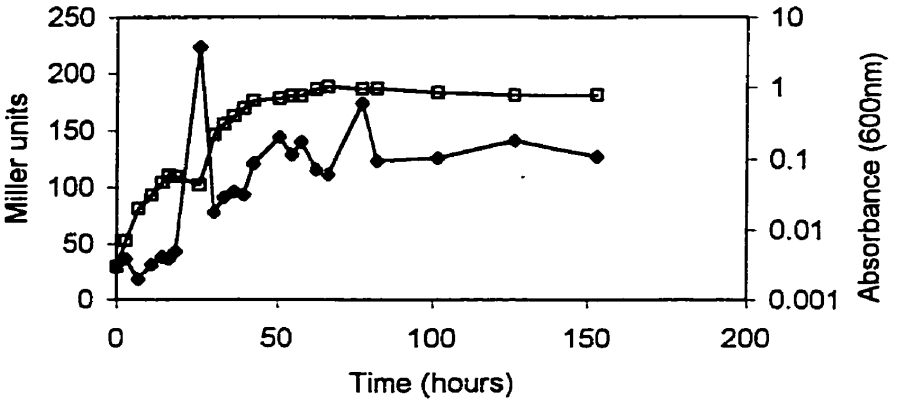

Glucose

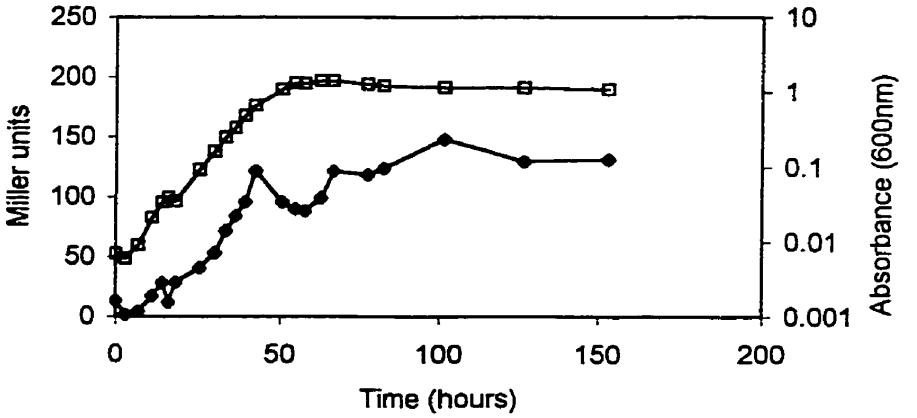

Figure 3.15. Comparison of growth kinetics of the wild-type strain and representative mutants on different carbon sources. Strains used were Rm1021 (wild type), Rm11134 (*acsA7*::Tn*5*), Rm11382 (*acsB*::Tn*5*) and Rm11364 (*acsA7*::Tn*5*, *acsB*::Tn*5*-233). Carbon sources were used at the following concentrations (mM): Glucose, 10; Acetate, 30; Acetoacetate, 15; 3-Hydroxybutyrate, 15. The growth of each culture was followed for 170 hours or until stationary phase was reached. ♦, wild type; ■, *acsA*; ▲, *acsB*; ×, *acsA acsB*.

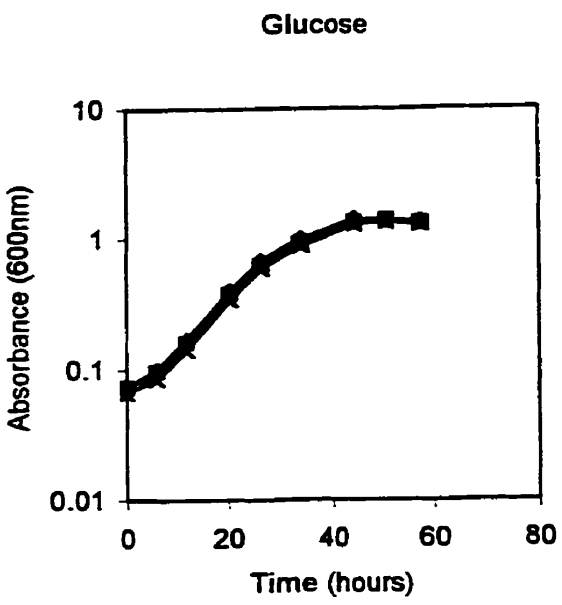
Glucose
Absorbance (600nm)
10
1
0.1
0.01
0
20
40
60
80
Time (hours)

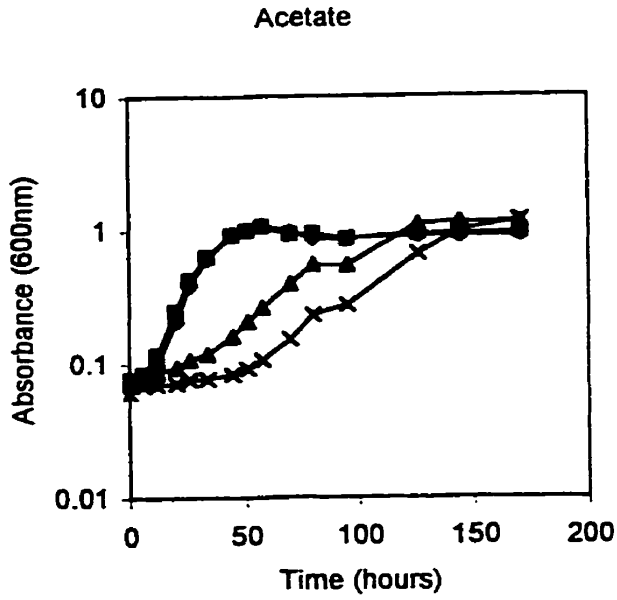
Acetate
Absorbance (600nm)
10
1
0.1
0.01
0
50
100
150
200
Time (hours)

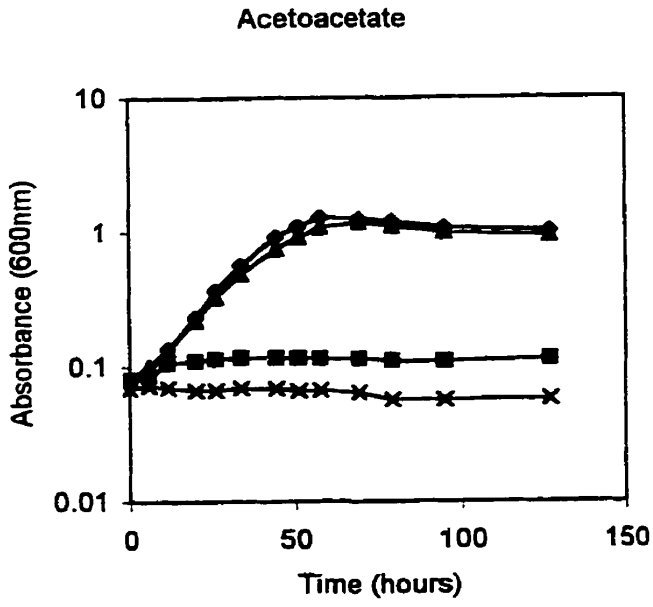
Acetoacetate
Absorbance (600nm)
10
1
0.1
0.01
0
50
100
150
Time (hours)

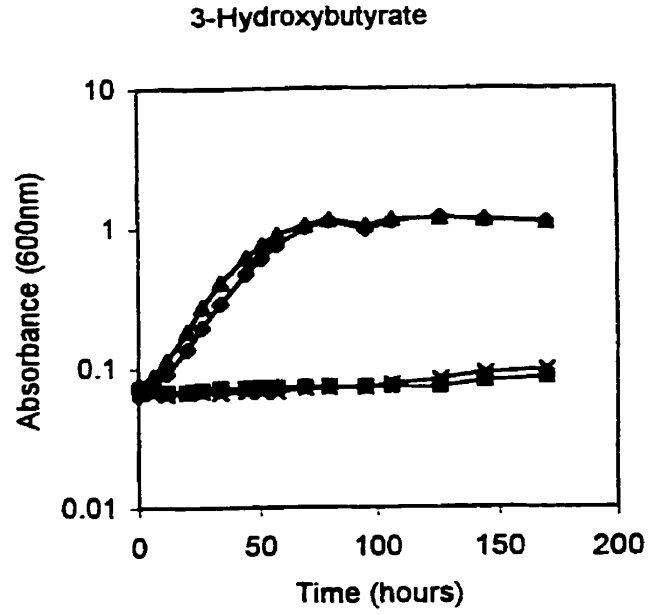
3-Hydroxybutyrate
Absorbance (600nm)
10
1
0.1
0.01
0
50
100
150
200
Time (hours)

Figure 3.16. Acetyl-CoA synthetase (ACS) and acetoacetyl-CoA synthetase (AACS) activities in cells of wild type and representative mutants grown on 15 mM M9 glucose. Values represent average specific activity in crude extracts ± SE of triplicate assays. ACS and AACS were assayed using standard methods as described in Materials and Methods. Strains used were Rm1021 (wild type), Rm11134 (*acsA7*::Tn*5*), Rm11382 (*acsB*::Tn*5*) and Rm11364 (*acsA7*::Tn*5*, *acsB*::Tn*5*-233).

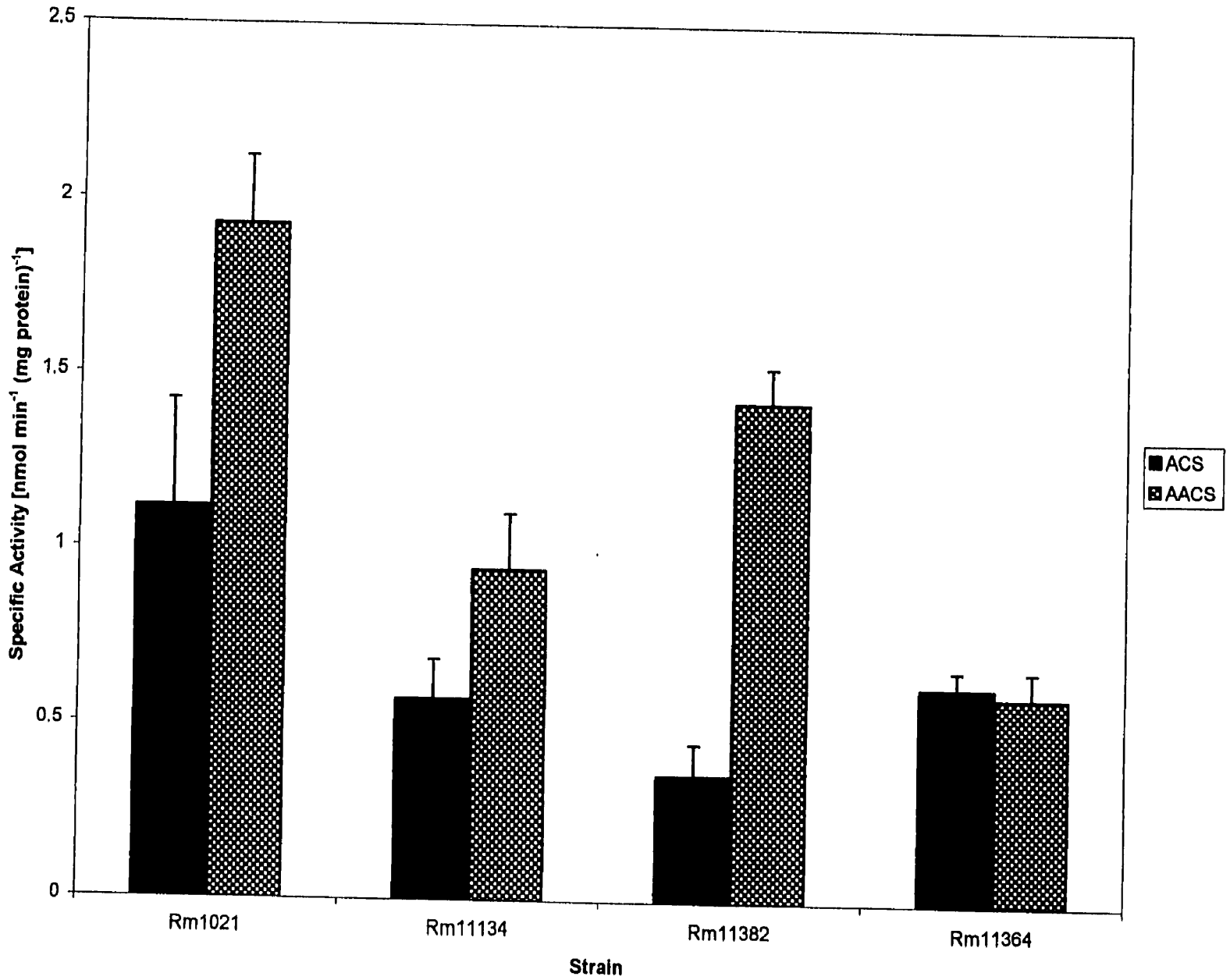
2.5
2
1.5
1
0.5
0
Specific Activity [nmol min-1 (mg protein)-1]
Rm1021
Rm11134
Rm11382
Rm11364
Strain
ACS
AACS

CHAPTER 4
DISCUSSION AND CONCLUSION

DISCUSSION

This investigation has identified at least three genes involved in acetate metabolism. Metabolism of acetate has been reviewed in *E. coli*, *S. typhimurium* and *S. cerevisiae*. In all cases, growth on acetate required the induction of the *aceBAK* operon. This operon encodes the metabolic and regulatory enzymes of the glyoxylate shunt. While the glyoxylate shunt enzymes are present in *S. meliloti*, the importance of the bypass in this organism is not very clear at this stage. Some acetate utilization mutants described in this study did carry lesions in genes encoding enzymes of the TCA cycle and gluconeogenesis. We also expected to find mutations in genes encoding enzymes of the glyoxylate shunt, but did not. There may be alternate routes in this organism that perform a similar function. The *pod* and *hemN* genes have not previously been shown to be involved in acetate metabolism. There is still not enough data to provide an interpretation as to why these *pod* and *hemN* mutations give an Ace$^-$ phenotype. It is possible that these mutations are polar on downstream genes and these may be responsible for the observed phenotype.

All the mutants without defects in gluconeogenesis were true acetate utilization mutants, and were not impaired in their capacity to compete with the wild type for growth under conditions of fluctuating carbon availability. It should be noted that the growth characteristics of mutants within group IV were not the same (see Table 3.1). Complementation tests (Table 3.3) were not consistent either. Nonetheless, the genes in this group are linked and may be related somehow. This is an interesting group to follow up. Cell free extracts from one mutant in this group had double the isocitrate lyase activity of the wild type.

If the glyoxylate bypass is the most important pathway in acetate metabolism, why were no glyoxylate shunt mutants obtained? In free-living *S. meliloti*, malate synthase is constitutively expressed and isocitrate lyase is inducible in acetate-grown cells (75), while *S. meliloti* bacteroids have low levels of malate synthase activity and insignificant levels of isocitrate lyase (34). It is possible that *S. meliloti* has alternate pathways that could potentially assimilate acetate, and the glyoxylate shunt is not as

essential as it is in *E. coli* for growth on acetate. The presence of alternate pathways to catabolize acetate in organisms that lack glyoxylate shunt enzymes has been suggested (49, 54, 67) but there is still insufficient data to support this. There could also be more than one copy of the genes encoding isocitrate lyase and malate synthase. There are organisms that possess multiple copies of isocitrate lyase or malate synthase (50, 52, 98, 116) but in all cases only one form is induced on acetate. On the other hand, the glyoxylate shunt may be so important that any mutations are lethal.

Sequence alignment of the two *acs* genes show how similar the aligned regions are to each other. However, the growth phenotype and enzyme activities (ACS and AACS) of the two *acs* mutants were not the same. The ACS and AACS also differ in their substrate specificities. The presence of two distinct Acs enzymes, with different substrate specificities, immunological and regulatory properties, has been reported in the organisms *Pyrococcus furiosus* and *S. cerevisiae* (71, 96).

The growth patterns of the *acsB* mutant (its growth on low concentrations of acetate only) are consistent with the results of *E. coli* and *Bacillus subtilis*, two organisms that utilize both the ACS and Ack-Pta pathway for acetate activation (48, 65). It has been suggested that ACS cannot convert acetate at a rate that is sufficient to reduce the toxicity associated with high concentrations of acetate. It is possible that the ACS pathway is the central pathway used for acetate utilization in *S. meliloti* and the Ack-Pta pathway acts in both acetate activation as well as acetate excretion. The fact that this mutant is able to grow on acetoacetate and 3-hydroxybutyrate indicates that these four-carbon compounds are not metabolized via the ACS pathway. Also observed in Figure 3.5 is that the lower the concentration of acetate, the less time it takes for the cells to adapt to the medium (shorter lag period). The ability of *S. meliloti* 104A14, another wild-type strain, to grow on organic acids depended on the pH of the medium, acid species and organic acid concentration (85). These factors affected the internal pH of the cells, and growth was found to be inhibited if the internal pH dropped below 7.0. It may therefore be advantageous for the cells to possess both acetate activation pathways so that the cells may grow across a wider range of acetate concentrations.

Since acetate can also be activated via the Ack-Pta pathway, the activity of these two enzymes might have interfered with the ACS assay. Why does the double mutant

(*acsA acsB*), have a higher ACS activity than the two single mutants? There are two possibilities:

If there is a third pathway for acetate activation when the two known pathways for acetate activation are non-functional, then perhaps AACS is needed to activate the Ack-Pta pathway. In wild-type cells both pathways would be operational. In the single mutants, only one pathway operates. From the results, it seems that ACS has a higher affinity for acetate than the other two enzymes. When there is no Ack-Pta and ACS activity (as in the double mutant), there might be another as yet unknown pathway for acetate activation. This would enable the double mutant to grow on acetate although with a longer lag period. The growth phenotype of a triple mutant (*acsA acsB ack*) on acetate may help verify this.

In the second case, ACS and AACS might be weak repressors of the Ack-Pta pathway. AACS may have an additional role of enhancing ACS activity. In the AcsA mutant, only the Ack-Pta would then be operational. In the AcsB mutant, there is no ACS activity and the Ack-Pta pathway is negatively regulated by AACS. In the double mutant, the Ack-Pta pathway dominates, as the two repressors may be absent. Growth of the double mutant on a range of acetate concentrations might be instructive.

Assaying the extracts of these strains for Ack and Pta activity might give us a better understanding of how the acetate is activated in the *acsA acsB* mutant. On the other hand, the problem may not be high activities in mutants, rather, low activities in the wild type. Previous enzyme studies in our lab did show higher ACS activity on glucose than on acetate, acetoacetate and 3-hydroxybutyrate medium (13). Perhaps higher activities would have been observed if a mixed carbon source, which included acetate, was used as growth substrate.

A mutant in group IV had mutations in the *hemN* gene, which encodes the anaerobic coproporphyrinogen III oxidase. Heme and modified derivatives are cofactors for a number of important enzymes. Heme synthesis occurs in 10 steps starting from glutamate. Coproporphyrinogen synthesis is a late step in the heme biosynthesis pathway (53). Coproporphyrinogen oxidation involves the conversion of the propionyl groups on the coproporphyrinogen III into vinyl groups. The reaction is an oxidative decarboxylation and requires an electron acceptor. Coproporphyrinogen III oxidases in

eukaryotes have an absolute requirement for oxygen. In bacteria there are two types of coproporphyrinogen III oxidases that can work aerobically and anaerobically. In *E. coli* the aerobic coproporphyrinogen oxidase is encoded by *hemF*, and the anaerobic coproporphyrinogen oxidase by *hemN* (111). In *S. typhimurium* the *hemN* can function both aerobically and anaerobically (120). There are a number of possibilities for the Ace$^-$ phenotype of the *hemN* mutant. The insertion could be producing a polar mutation on a downstream gene. Alternatively, the product of the *hemN* gene could act as a cofactor specifically for a component of an acetate utilization pathway. Another explanation would be that a heme protein substitute is not expressed on acetate. Since *hemN* encodes an oxidase, perhaps cells that are defective in this enzyme have high NADH/NAD$^+$ ratios, which in turn inhibit enzymes like citrate synthase and malate dehydrogenase, shared by the TCA cycle and the glyoxylate shunt. Enzyme assays of this strain may help clear up this ambiguity.

Even though mutations in *ace1* and *ace4* are 80% linked by transduction (about 9 kb apart), complementation studies indicate that the mutations are probably not allelic but in distinct loci. The complementing fragment in pZT2 most likely carries both genes and the complementing fragment in pZT8 may only bear the region that complements the *ace4* mutation. While not likely in the isocitrase lyase gene, we have not eliminated malate synthase as a possibility for either.

RmG274 has both the *pod* and the suppressor mutation *spk*. Rm11200 (*ace13*::Tn5) isolated in our laboratory has a mutation in the *pod* gene. Transduction experiments indicated that the *spk* mutation in RmG274 is somehow suppressing the Ace$^-$ phenotype of the *pod* mutant. This explained the different acetate phenotypes of these two strains. The growth curve experiments with RmG274, RmG139, Rm11200 and *pckA* mutants suggested that the *pod* gene plays a role in the suppression of the succinate phenotype in a *pckA* mutant. Does the *pckA* gene play a role in the suppression of the Ace phenotype in the *pod* mutant? If it does, could Pck be the suppressor? We could try to isolate suppressors of the *pod* mutant by selecting for spontaneous mutations that rescue the Ace$^-$ phenotype of the *pod* mutant on M9 acetate, and then check if these second-site mutations map near *pckA*.

The expression of genes involved in carbon source utilization is often regulated in a manner that reflects the availability of substrate. The expression of *pckA* was induced on gluconeogenic substrates such as succinate and arabinose (83). The expression of *pod* did not appear to depend on growth phase or the carbon source used for growth. The sudden drop at OD_{600} on M9 succinate at the onset of the log phase (Figure 3.13) suggests an experimental error. This drop may have affected the β-galactosidase activity since the cell density is taken into consideration when calculating the β-galactosidase activity (expressed in Miller Units). However, the error may not be sufficient to account for the magnitude (i.e four-fold) of the increase. The expression level of the *pckA* gene on acetate as a sole carbon source has not been determined, and therefore it is not known whether *pckA* expression is reduced on acetate. It is possible that the balance of pyruvate ↔ PEP is more critical during growth on acetate, and PPDK plays a role in achieving and maintaining this balance.

CONCLUSION

This study was originally pursued with the goal of characterizing genes encoding enzymes of the glyoxylate shunt. However, the results do indicate a possibility that *S. meliloti* has alternate pathways that could potentially catabolize acetate. It also tells us that there is still much to learn about the pathways this organism can use for intermediary carbon metabolism.

For a better understanding of acetate metabolism in *S. meliloti*, more mutants will have to be characterized. We need to study genes that are required for growth on acetate and also genes that are induced during growth on acetate. Each mutant in group IV may need to be characterized and this group may need reclassification. Since we were particularly interested in characterizing the genes that encode the enzymes of the glyoxylate shunt and determining their regulation, one approach to characterize glyoxylate shunt mutations would be to construct mutants using the DNA sequence information available for isocitrate lyase and malate synthase from other organisms. If glyoxylate shunt mutations are lethal, one way to isolate them would be to perform mutagenesis with the conditional mutation generating transposon, Tn5-tac (73).

This study indicates that the mechanisms used to metabolize two-carbon compounds such as acetate in *S. meliloti* are probably different from that used by enterics. We are just beginning to understand the potential impact of acetate use on carbon metabolism. However, much remains to be learned about the role and function of acetate in rhizobia.

REFERENCES

1. **Altschul, S. F., T. L. Madden, A. A. Schäffer, Z. Zhang, W. Miller, and D. Lipman.** 1997. Gapped BLAST and PSI-BLAST: a new generation of protein database search programs. Nuc. Acids Res. **25:**3389-3402.

2. **Anderson, A. J., and E. A. Dawes.** 1990. Occurrence, metabolism, metabolic role, and industrial uses of bacterial polyhydroxyalkanoates. Microbiol. Rev. **54:**450-472.

3. **Aneja, P., G.-Q. Cai, B. T. Driscoll, and T. C. Charles.** 1998. *Sinorhizobium meliloti* mutant studies demonstrate an important role for polyhydroxyalkanoate deposits in competition for nodulation and for competitive growth. Presented at the Eighth International Symposium on Microbial Ecology, Halifax.

4. **Arwas, R., I. A. McKay, F. R. P. Rowney, M. J. Dilworth, and A. R. Glenn.** 1985. Properties of organic acid utilization mutants of *Rhizobium leguminosarum* strain 300. J. Gen. Microbiol. **131:**2059-2066.

5. **Atlas, R. M.** 1993. Handbook of microbiological media. CRC Press Inc., Boca Raton, Florida.

6. **Ausubel, F.** 1989-94. Current Protocols in Molecular Biology. Greene Pub. Associates, Inc. and John Wiley & Sons, Inc., New York.

7. **Ausubel, F. M., R. Brent, R. E. Kingston, D. D. Moore, J. G. Seidman, J. A. Smith, and K. Struhl.** 1997. Current protocols in molecular biology. John Wiley & Sons, New York, N.Y.

8. **Berg, C. M., and D. E. Berg.** 1987. Uses of transposable elements and maps of known insertions, p. 1071-1109. *In* F. C. Niedhardt, J. L. Ingraham, K. B. Low, B. Magasanik, M. Schaechter, and H. E. Umbarger (ed.), *Escherichia coli* and *Salmonella typhimurium*: Cellular and Molecular Biology. American Society for Microbiology, Washington, D.C.

9. **Beringer, J. E.** 1974. R-factor transfer in *Rhizobium leguminosarum*. J. Gen. Microbiol. **84:**188-198.

10. **Beringer, J. E., J. L. Beynon, A. V. Buchanan-Wollaston, and A. W. B. Johnston.** 1978. Transfer of the drug resistance transposon Tn*5* to *Rhizobium*. Nature. **276:**633-634.

11. **Bradford, M. M.** 1976. A rapid and sensitive method for the quantitation of microgram quantities of protein utilizing the principle of protein-dye binding. Anal. Biochem. **72:**248-254.

12. **Brown, T. D. K., M. C. Jones-Mortimer, and H. L. Kornberg.** 1977. The enzymatic interconversion of acetate and acetyl-coenzyme A in *Escherichia coli*. J. Gen. Microbiol. **102:**327-336.

13. **Butler, S.** 1996. The effect of different carbon sources on the specific activity of enzymes of the acetate activation pathways, the glyoxylate shunt, the TCA cycle and the poly-β-hydroxybutyrate cycle. Undergraduate research project. McGill University, Montreal.

14. **Cai, G.-Q., and T. Charles.** 1996. At least five chromosomal loci are required for growth of *Rhizobium meliloti* on acetoacetate. Presented at the 96th General Meeting of the American Society for Microbiology, New Orleans, LA, May 19-23.

15. **Cai, G.-Q., and T. C. Charles.** 1996. Identification and characterization of a PHB degradation pathway locus in *Rhizobium meliloti.* Presented at the 8th International Congress, Molecular Plant-Microbe Interactions, Knoxville, TN, July 14-19.

16. **Cai, G.-Q., B. T. Driscoll, and T. C. Charles.** 1998. Involvement of gene encoding (aceto)acetyl-CoA synthetase (*acsA*) in the degradation of acetoacetate and 3-hydroxybutyrate by *Sinorhizobium meliloti.* Presented at the 48th Annual Meeting of Canadian Society of Microbiologists, Guelph.

17. **Charles, T. C., G.-Q. Cai, and P. Aneja.** 1997. Megaplasmid and chromosomal loci for the PHB degradation pathway in *Rhizobium* (*Sinorhizobium*) *meliloti*. Genetics. **146:**1211-1220.

18. **Charles, T. C., and E. W. Nester.** 1993. A chromosomally encoded two-component sensory transduction system is required for virulence of *Agrobacterium tumefaciens*. J. Bacteriol. **175:**6614-6625.

19. **Chistoserdova, L. V., and M. E. Lidstrom.** 1996. Molecular characterization of a chromosomal region involved in the oxidation of acetyl-CoA into glyoxylate in the ICL$^-$ methylotroph, *Methylobacterium extorquens* AM1. Microbiology. **142:**1459-1468.

20. **Chung, T., J. Klumpp, and D. C. LaPorte.** 1988. Glyoxylate bypass operon of *Escherichia coli*: cloning and determination of the functional map. J. Bacteriol. **170:**386-392.

21. **Clark, D. P., and J. E. Cronan Jr.** 1996. Two-carbon compounds and fatty acids as carbon sources, p. 343-357. *In* F. C. Neidhardt, R. Curtiss III, J. L. Ingraham, E. C. C. Lin, J. Brooks Low, K, B. Magasanik, W. S. Reznikoff, M. Riley, M. Schaechter, and H. E. Umbarger (ed.), *Escherichia coli* and *Salmonella typhimurium* : Cellular and Molecular Biology. American Society for Microbiology, Washington, D.C.

22. **Cortay, J. C., F. Bleicher, C. Rieul, H. C. Reeves, and A. J. Cozzone.** 1988. Nucleotide sequence and expression of the *aceK* gene coding for isocitrate dehydrogenase kinase/phosphatase in *Escherichia coli*. J. Bacteriol. **170:**89-97.

23. **Cortay, J. C., D. Negre, A. Galinier, B. Duclos, G. Perriere, and A. J. Cozzone.** 1991. Regulation of the acetate operon in *Escherichia coli*: purification and functional characterization of the IclR repressor. EMBO J. **10:**675-679.

24. **Cozzone, A. J.** 1998. Regulation of acetate metabolism by protein phosphorylation in enteric bacteria. Annu Rev Microbiol. **52:**127-164.

25. **Cronan Jr., J. E., and D. E. LaPorte.** 1996. Tricarboxylic acid cycle and glyoxylate bypass, p. 206-216. *In* F. C. Neidhardt, R. Curtiss III, J. L. Ingraham, E. C. C. Lin, J. Brooks Low, K, B. Magasanik, W. S. Reznikoff, M. Riley, M. Schaechter, and H. E. Umbarger (ed.), *Escherichia coli* and *Salmonella typhimurium*: Cellular and Molecular Biology. American Society for Microbiology, Washington, DC.

26. **Dailey, F. E., and J. E. Cronan, Jr.** 1986. Acetohydroxy acid synthase I, a required enzyme for isoleucine and valine biosynthesis in *Escherichia coli* K-12 during growth on acetate as the sole carbon source. J. Bacteriol. **165:**453-460.

27. **Dailey, F. E., J. E. Cronan, Jr., and S. R. Maloy.** 1987. Acetohydroxy acid synthase I is required for isoleucine and valine biosynthesis by *Salmonella typhimurium* LT2 during growth on acetate or long-chain fatty acids. J. Bacteriol. **169:**917-919.

28. **De Vos, G. F., G. C. Walker, and E. R. Signer.** 1986. Genetic manipulations in *Rhizobium meliloti* utilizing two new transposon Tn*5* derivatives. Mol. Gen. Genet. **204:**485-491.

29. **DeFelice, M., T. Newman, and M. Levinthal.** 1978. Regulation of synthesis of the acetohydroxy acid synthase I isozyme in *Escherichia coli* K-12. Biochim. Biophys. Acta. **541:**9-17.

30. **Diehl, P., and B. A. McFadden.** 1994. The importance of four histidine residues in isocitrate lyase from *Escherichia coli*. J. Bacteriol. **176:**927-931.

31. **Dixon, G. H., and H. L. Kornberg.** 1959. Assay method for key enzymes of the glyoxylate shunt. Biochem. J. **72:**3p.

32. **Driscoll, B. T., and T. M. Finan.** 1997. Properties Of NAD(+)- and NADP(+)-dependent malic enzymes of *Rhizobium (Sinorhizobium) meliloti* and differential expression of their genes in nitrogen-fixing bacteroids. Microbiology. **143:**489-498.

33. **Duncan, M. J., and D. G. Fraenkel.** 1979. α-Ketoglutarate dehydrogenase mutant of *Rhizobium meliloti*. J. Bacteriol. **137:**415-419.

34. **Dunn, M. F.** 1998. Tricarboxylic acid cycle and anaplerotic enzymes in rhizobia. FEMS Microbiol. Rev. **22:**105-123.

35. **Eikmanns, B. J., D. Rittmann, and M. Sahm.** 1995. Cloning, sequencing analysis, expression, and inactivation of the *Corynebacterium glutamicum icd* gene encoding isocitrate dehydrogenase and biochemical characterization of the enzyme. J. Bacteriol. **177:**774-782.

36. **Engelke, T., M. N. Jagadish, and A. Puhler.** 1987. Identification and sequence analysis of *Rhizobium meliloti* mutants defective in C_4-dicarboxylate transport. J. Gen. Microbiol. **133:**3019-3029.

37. **Finan, T. M.** Unpublished.

38. **Finan, T. M., E. K. Hartwieg, K. LeMieux, K. Bergman, G. C. Walker, and E. R. Signer.** 1984. General transduction in *Rhizobium meliloti*. J. Bacteriol. **159:**120-124.

39. **Finan, T. M., B. Kunkel, G. F. DeVos, and E. R. Signer.** 1986. Second symbiotic megaplasmid in *Rhizobium meliloti* carrying exopolysaccharide and thiamine synthesis genes. J. Bacteriol. **167:**66-72.

40. **Finan, T. M., I. Oresnik, and A. Bottacin.** 1988. Mutants of *Rhizobium meliloti* defective in succinate metabolism. J. Bacteriol. **170:**3396-3403.

41. **Finan, T. M., J. M. Wood, and D. C. Jordan.** 1983. Symbiotic properties of C_4-dicarboxylic acid transport mutants of *Rhizobium leguminosarum*. J. Bacteriol. **154:**1403-1413.

42. **Friedman, A. M., S. R. Long, S. E. Brown, W. J. Buikema, and F. M. Ausubel.** 1982. Construction of a broad host range cloning vector and its use in the genetic analysis of *Rhizobium* mutants. Gene. **18:**289-296.

43. **Gardiol, A., A. Arias, C. Cervenansky, and G. Martinez-Dretz.** 1982. Succinate dehydrogenase mutant of *Rhizobium meliloti*. J. Bacteriol. **151:**1621-1623.

44. **Garnak, M., and H. C. Reeves.** 1979. Phosphorylation of isocitrate dehydrogenase of *Escherichia coli*. Science. **203:**1111-1112.

45. **Gish, W., and D. J. States.** 1993. Identification of protein coding regions by database similarity search. Natural Genetics **3:**266-272.

46. **Glazebrook, J., and G. C. Walker.** 1991. Genetic techniques in *Rhizobium meliloti*. Methods Enzymol. **204:**398-418.

47. **Green, L. S., D. B. Karr, and D. W. Emerich.** 1998. Isocitrate dehydrogenase and glyoxylate cycle enzyme activities in *Bradyrhizobium japonicum* under various growth conditions. Arch. Microbiol. **169:**445-451.

48. **Grundy, F. J., D. A. Waters, T. Y. Takova, and T. M. Henkin.** 1993. Identification of genes involved in utilization of acetate and acetoin in *Bacillus subtilis*. Mol. Microbiol. **10:**259-271.

49. **Han, L., and K. A. Reynolds.** 1997. A novel alternate anaplerotic pathway to the glyoxylate cycle in streptomycetes. J. Bacteriol. **179:**5157-5164.

50. **Harrop, L. C., and H. L. Kornberg.** 1966. The role of isocitrate lyase in the metabolism of algae. Proc. R. Soc. London. **166**(B)**:**11-29.

51. **Hennecke, H.** 1998. Rhizobial respiration to support symbiotic nitrogen fixation. Kluwer Academic Publishers, Dordrecht, the Netherlands.

52. **Hillier, S., and W. T. Charnetzky.** 1981. Glyoxylate bypass enzymes in *Yersinia* species and multiple forms of isocitrate lyase in *Yersinia pestis*. J. Bacteriol. **145:**452-458.

53. **Hippler, B., G. Homuth, T. Hoffman, C. Hungerer, W. Schumann, and D. Jahn.** 1997. Characterization of *Bacillus subtilis hemN*. J. Bacteriol. **179:**7181-7185.

54. **Holms, W. H.** 1986. Evolution of the glyoxylate bypass in *Escherichia coli* - an hypothesis which suggests an alternative to the Krebs cycle. FEMS Microbiol. Lett. **34:**123-127.

55. **Ikeda, T. P., and D. C. LaPorte.** 1991. Isocitrate dehydrogenase kinase/phosphatase:*aceK* alleles that express kinase but not phosphatase activity. J. Bacteriol. **173:**1801-1806.

56. **Ishii, A., S. Imagawa, N. Fukunaga, S. Sasaki, O. Minowa, et al.** 1987. Isozymes of isocitrate dehydrogenase from an obligately psychrophilic bacterium, *Vibrio* sp. strain ABE-1:purification and modulation of activities by growth conditions. J. Biochem. **102:**1489-1498.

57. **Iuchi, S., D. C. Cameron, and E. C. C. Lin.** 1989. A second global regulatory gene (*arcB*) mediating repression of enzymes in aerobic pathways of *Escherichia coli*. J. Bacteriol. **171:**868-873.

58. **Iuchi, S., Z. Matsuda, T. Fujiwara, and E. C. C. Lin.** 1988. *arcA* (*dye*), a global regulatory gene in *Escherichia coli* mediating repression of enzymes in aerobic pathways. Proc. Natl. Acad. Sci. USA. **85:**1888-1892.

59. **Jackson, E. K., and H. J. Evans.** 1966. Propionate in heme biosynthesis in soybean nodules. Plant Physiol. **41:**1330-1336.

60. **Johnson, G. V., H. J. Evans, and T. Ching.** 1966. Enzymes of the glyoxylate cycle in rhizobia and nodules of legumes. Plant Physiol. **41:**1330-1336.

61. **Kahn, M. L., M. Mortimer, K. S. Park, and W. Zhang.** 1995. Carbon metabolism in the rhizobium-legume symbiosis, p. 525-532. *In* I. A. Tikhonovich, N. A. Proporov, V. I. Romanov, and W. E. Newton (ed.), Nitrogen fixation: fundamentals and applications. Kluwer Academic Publishers, Dordrecht, The Netherlands.

62. **Klein, S., K. Lohmann, R. Clover, G. C. Walker, and E. R. Signer.** 1992. A directional, high-frequency chromosomal localization system for genetic mapping in *Rhizobium meliloti*. J. Bacteriol. **174:**324-326.

63. **Kornberg, H. L.** 1966. Anaplerotic sequences and their role in metabolism. Essays Biochem. **11:**1-31.

64. **Kornberg, H. L.** 1966. The role and control of the glyoxylate cycle in *Escherichia coli*. Biochem. J. **99:**1-11.

65. **Kumari, S., R. Tishel, M. Eisenbach, and A. J. Wolfe.** 1995. Cloning, characterization, and functional expression of *acs*, the gene which encodes acetyl coenzyme A synthetase in *Escherichia coli*. J. Bacteriol. **177:**2878-2886.

66. **LaPorte, D. C., and T. Chung.** 1985. A single gene codes for the kinase and phosphatase which regulate isocitrate dehydrogenase. J. Biol. Chem. **260:**15291-15297.

67. **LaPorte, D. C., P. E. Thorsness, and D. E. Koshland.** 1985. Compensatory phosphorylation of isocitrate dehydrogenase: a mechanism for adaptation to the intracellular environment. J. Biol. Chem. **260:**10563-10568.

68. **LaPorte, D. C., K. Walsh, and D. E. Koshland Jr.** 1984. The branch point effect: ultrasensitivity and subsensitivity to metabolic control. J. Biol. Chem. **259:**14068-14075.

69. **LeVine, S. M., F. Ardeshir, and G. F.-L. Ames.** 1980. Isolation and characterization of acetate kinase and phosphotransacetylase mutants of *Escherichia coli* and *Salmonella typhimurium*. J. Bacteriol. **143:**1081-1085.

70. **Leyland, M. L., and D. J. Kelly.** 1991. Purification and characterization of a monomeric isocitrate dehydrogenase with dual coenzyme from the photosynthetic bacterium *Rhodomicrobium vannielli*. Eur. J. Biochem. **202:**85-93.

71. **Mai, X., and M. W. W. Adams.** 1996. Purification and characterization of two reversible and ADP-dependent acetyl coenzyme A synthetases from the hyperthermophilic archaeon *Pyrococcus furiosus*. J. Bacteriol. **178:**5897-5903.

72. **Maloy, S. R., M. Bohlander, and W. D. Nunn.** 1980. Elevated levels of glyoxylate shunt enzymes in *Escherichia coli* strains constitutive for fatty acid degradation. J. Bacteriol. **143:**720-725.

73. **Maloy, S. R., J. E. Cronan Jr., and D. Freifelder.** 1994. Microbial Genetics, Second ed. Jones and Bartlett Publishers, Boston.

74. **Maloy, S. R., and W. D. Nunn.** 1982. Genetic regulation of the glyoxylate shunt in *Escherichia coli* K-12. J. Bacteriol. **149:**173-180.

75. **Mandal, N., and P. K. Chakrabartty.** 1992. Regulation of enzymes of glyoxylate pathway in root-nodule bacteria. J. Gen. Appl. Microbiol. **38:**417-427.

76. **McCammon, M. T.** 1996. Mutants of *Saccharomyces cerevisiae*with defects in acetate metabolism: Isolation and characterization of Acn$^-$ mutants. Genetics. **144:**57-69.

77. **McDermott, T. R., S. M. Griffith, C. P. Vance, and P. H. Graham.** 1989. Carbon metabolism in *Bradyrhizobium japonicum* bacteroids. FEMS Microbiol. Rev. **63:**327-340.

78. **McDermott, T. R., and M. L. Kahn.** 1992. Cloning and mutagenesis of the *Rhizobium meliloti* isocitrate dehydrogenase gene. J. Bacteriol. **174:**4790-4797.

79. **Meade, H. M., S. R. Long, G. B. Ruvkun, S. E. Brown, and F. M. Ausubel.** 1982. Physical and genetic characterization of symbiotic and auxotrophic mutants of *Rhizobium meliloti* induced by transposon mutagenesis. J. Bacteriol. **149:**114-122.

80. **Miller, J. H.** 1972. Experiments in molecular genetics. Cold Spring Harbor Laboratory, Cold Spring Harbor, N.Y.

81. **Oresnik, I. J., L. A. Pacarynuk, S. A. P. O'Brien, C. K. Yost, and M. F. Hynes.** 1998. Plasmid-encoded catabolic genes in *Rhizobium leguminosarum* bv. *trifolii*: Evidence for a plant-inducible rhamnose locus involved in competition for nodulation. Molecular Plant-Microbe Interactions. **11:**1175-1185.

82. **Østerås, M., B. T. Driscoll, and T. M. Finan.** 1997. Increased pyruvate orthophosphate dikinase activity results in an alternative gluconeogenic pathway in *Rhizobium (Sinorhzobium) meliloti*. Microbiology. **143:**1639-1648.

83. **Østerås, M., B. T. Driscoll, and T. M. Finan.** 1995. Molecular and expression analysis of the *Rhizobium meliloti* phosphoenolpyruvate carboxykinase (*pckA*) gene. J. Bacteriol. **177:**1452-1460.

84. **Østerås, M., J. Stanley, and T. M. Finan.** 1995. Identification of Rhizobium-specific intergenic mosaic elements within an essential two-component regulatory system of *Rhizobium* species. J. Bacteriol. **177:**5485-5494.

85. **Perez-Galdona, R., and M. L. Kahn.** 1994. Effect of organic acids and low pH on *Rhizobium meliloti* 104A14. Microbiology. **140:**1231-1235.

86. **Pocalyko, D. J., L. J. Carroll, B. M. Martin, P. C. Babbitt, and D. Dunaway-Mariano.** 1990. Analysis of sequence homologies in plant and bacterial pyruvate phosphate dikinase, enzyme I of the bacterial phosphoenolpyruvate: sugar phosphotransferase system and other PEP-utilizing enzyme. Identification of potential catalytic and regulatory motifs. Biochem. **29:**10757-10765.

87. **Povolo, S., R. Tombolini, A. Morea, A. J. Anderson, S. Casella, and M. P. Nuti.** 1994. Isolation and characterization of mutants of *Rhizobium meliloti* unable to synthesize poly-β-hydroxybutyrate (PHB). Can. J. Microbiol. **40:**823-829.

88. **Prescott, L. M., J. P. Harley, and D. A. Klein.** 1993. Microbiology, Second ed. Wm. C. Brown Publishers.

89. **Ramseier, T. M., S. Bledig, V. Michotey, R. Feghali, and M. H. Saier Jr.** 1995. The global regulatory protein, FruR, modulates the direction of carbon flow in *Escherichia coli*. Mol. Microbiol. **16:**1157-1161.

90. **Ramseier, T. M., D. Negre, J. C. Cortay, M. Scarabel, A. J. Cozzone, and M. H. Saier Jr.** 1993. *In vitro* binding of the pleiotrophic transcriptional regulatory protein, FruR, to the *fru*, *pps*, *ace*, *pts* and *icd* operons of *Escherichia coli* and *Salmonella typhimurium*. J. Mol. Biol. **234:**28-44.

91. **Rawsthorne, S., F. R. Minchin, R. J. Summerfield, C. Cookson, and J. Coombs.** 1980. Carbon and nitrogen metabolism in legume root nodules. Phytochemistry. **19:**341-355.

92. **Ronson, C. W., P. Lyttleton, and J. G. Robertson.** 1981. C_4-dicarboxylate transport mutants of *Rhizobium trifolii* form ineffective nodules on *Trifolium repens*. Proc. Natl. Acad. Sci. USA. **82:**6231-6245.

93. **Ruvkun, G. B., and F. M. Ausubel.** 1981. A general method for site-directed mutagenesis in prokaryotes. Nature. **289:**85-88.

94. **Saier, M. H., T. M. Ramseier, and J. Reizer.** 1996. Regulation of carbon utilization. *In* F. C. Neidhardt, R. Curtiss III, J. L. Ingraham, E. C. C. Lin, J. Brooks Low, K, B. Magasanik, W. S. Reznikoff, M. Riley, M. Schaechter, and H. E. Umbarger (ed.), *Escherichia coli* and *Salmonella typhimurium*: Cellular and Molecular Biology. American Society for Microbiology, Washington, DC.

95. **Sambrook, J., E. F. Fritsch, and T. Maniatis.** 1989. Molecular cloning: a laboratory manual. Cold Spring Harbor Laboratory Press, Cold Spring Harbor, N.Y.

96. **Satyanarayana, T., A. D. Mandel, and H. P. Klein.** 1974. Evidence for two immunologically distinct acetyl coenzyme A synthetases in yeast. Biochim. Biophys. Acta. **341:**396-401.

97. **Simon, R., J. Quandt, and W. Klipp.** 1989. New derivatives of transposon Tn*5* suitable for mobilization of replicons, generation of operon fusions, and induction of genes in Gram-negative bacteria. Gene. **80:**161-169.

98. **Sjorgen, R. E., and A. H. Romano.** 1967. Evidence for multiple forms of isocitrate lyase in *Neurospora crassa*. J. Bacteriol. **93:**1638-1643.

99. **Smith, M. T., G. G. Preston, and D. W. Emerich.** 1994. Development of acetate and pyruvate metabolic enzyme activities in soybean nodules. Symbiosis. **17:**33-42.

100. **Stachel, S. E., G. An, C. Flores, and E. W. Nester.** 1985. A Tn*3* *lacZ* transposon for the random generation of beta-galactosidase gene fusions: application to the analysis of gene expression in *Agrobacterium*. EMBO J. **4:**891-898.

101. **Stadtman, E. C.** 1952. The purification and properties of phosphotransacetylase. J. Biol. Chem. **196:**527-534.

102. **Stowers, M. D.** 1985. Carbon metabolism in *Rhizobium* species. Annu. Rev. Microbiol. **39:**89-108.

103. **Streeter, J. G.** 1991. Transport and metabolism of carbon and nitrogen in legume nodules. Adv. Botan. Res. **18:**129-187.

104. **Stueland, C. S., K. R. Eck, K. T. Stieglbauer, and D. C. LaPorte.** 1987. Isocitrate dehydrogenase kinase/phosphatase exhibits and intrinsic adenosine triphosphatase activity. J. Biol. Chem. **262:**16095-16099.

105. **Summers, M. L., M. C. Denton, and T. R. McDermott.** 1999. Genes coding for phosphotransacetylase and acetate kinase in *Rhizobium meliloti* are in an operon that is induced by phophate stress and controlled by PhoB. J. Bacteriol. **181:**2217-2224.

106. **Summers, M. L., M. L. Kahn, and T. R. McDermott.** 1996. Phosphate stress inducible genes of *Rhizobium meliloti.* Presented at the 8th International Congress, Molecular Plant-Microbe Interactions, Knoxville, TN, July 14-19.

107. **Sunnarborg, A., D. Klumpp, T. Chung, and D. C. LaPorte.** 1990. Regulation of the glyoxylate bypass operon: cloning and characterization of *iclR*. J. Bacteriol. **172:**2642-2649.

108. **Thaha, Z.** 1994. Generation and characterization of acetate mutants of *Rhizobium meliloti* deficient in the enzymes of the glyoxylate shunt. Undergraduate research project. McGill University, Montreal.

109. **Thorsness, P. E., and D. E. Koshland Jr.** 1987. Inactivation of isocitrate dehydrogenase by phosphorylation is mediated by the negative charge of the phosphate. J. Biol. Chem. **262:**10422-10425.

110. **Tombolini, R., and M. P. Nuti.** 1989. Poly (β-hydoxyalkanoate) biosynthesis and accumulation by different *Rhizobium* species. FEMS Microbiol. Lett. **60:**299-304.

111. **Troup, B., C. Hungerer, and D. Jahn.** 1995. Cloning and characterization of the *Escherichia coli hemN* gene encoding the oxygen-independent coproporphyrinogen III oxidase. J. Bacteriol. **177:**3326-3331.

112. **Udvardi, M. K., and D. A. Day.** 1989. Electrogenic ATPase activity on the peribacteroid membrane of soybean (*Glycine max* L.) root nodules. Plant Physiol. **90:**982-987.

113. **Vance, C. P., and G. H. Heichel.** 1991. Carbon in N_2 fixation: Limitation or exquisite adaptation. Annu. Rev. Plant Physiol. Plant Mol. Biol. **42:**373-392.

114. **Walsh, K., and D. E. Koshland Jr.** 1984. Determination of flux through the branch point of two metabolic cycles. The tricarboxylic acid cycle and the glyoxylate shunt. J. Biol. Chem. **259:**9646-9654.

115. **Waters, J. K., B. L. Hughes II, L. C. Purcell, K. O. Gerhadt, T. P. Mawhinney, and D. W. Emerich.** 1998. Alanine, not ammonia, is excreted from N_2-fixing soybean nodules bacteroids. Proc. Natl. Acad. Sci. USA. **95:**12038-12042.

116. **Wegener, W. S., J. E. Schell, and A. H. Romano.** 1967. Control of malate synthase formation in *Rhizopus nigricans*. J. Bacteriol. **87:**156-161.

117. **Willis, L. B., and G. C. Walker.** 1998. The *phbC* (poly-β-hydroxybutyrate synthase) gene of *Rhizobium (Sinorhizobium) meliloti* and characterization of *phbC* mutants. Can. J. Microbiol. **44:**554-564.

118. **Wilson, R. B., and S. R. Maloy.** 1987. Isolation and characterization of *Salmonella typhimurium* glyoxylate shunt mutants. J. Bacteriol. **169:**3029-3034.

119. **Wu, T. T.** 1966. A model for three-point analysis of random general transduction. Genetics. **54:**405-410.

120. **Xu, K., and T. Elliot.** 1994. Cloning, DNA sequence, and complementation analysis of the *Salmonella typhimurium hemN* gene encoding encoding a putative oxygen-independent coproporphyrinogen III oxidase. J. Bacteriol. **176:**3196-3203.

121. **Yanisch-Perron, C., J. Vieira, and J. Messing.** 1985. Improved M13 phage cloning vectors and host strains: nucleotide sequences of the M13mp18 and pUC19 vectors. Gene. **33:**103-119.

122. **Yarosh, O. K., T. C. Charles, and T. M. Finan.** 1989. Analysis of C_4 - dicarboxylate transport genes in *Rhizobium meliloti*. Mol. Microbiol. **3:**813-823.